

PHOTOLYSIS OF SOME ORGANIC SULPHUR COMPOUNDS

**CENTRE FOR NEWFOUNDLAND STUDIES**

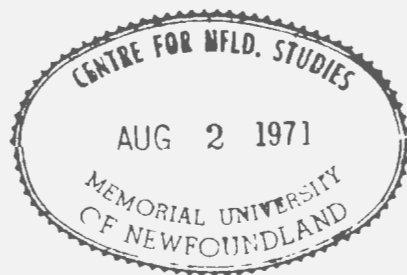
**TOTAL OF 10 PAGES ONLY  
MAY BE XEROXED**

**(Without Author's Permission)**

JOHN N. ATHERTON, B.SC.



25500





PHOTOLYSIS OF SOME ORGANIC SULPHUR COMPOUNDS

A Thesis

by



John N. Atherton B.Sc.

Submitted in partial fulfillment of the requirement for  
the degree of Master of Science.

March 1971

Memorial University  
of Newfoundland

This thesis has been examined and approved by

Dr. A.G. Fallis  
Department of Chemistry  
Memorial University of Newfoundland  
St. John's

Dr. B.A. Morrow  
Department of Chemistry  
University of Ottawa  
Ottawa

## ACKNOWLEDGEMENTS

The author wishes to express his sincere thanks to Dr. J.F. Ogilvie for his supervision of this work and to Dr. N.J. Gogan whose guidance with the E.S.R. experiments was invaluable. Thanks are also due to Dr. J.M.W. Scott for providing the CD<sub>3</sub>I sample and to Dr. H.J. Clase and Mr. T.H. Buckley for recording the Raman and N.M.R. spectra respectively.

Grateful acknowledgement is made to my wife for helping to prepare the manuscript and to Mrs. Carol Piercey for patiently typing this dissertation.

## PREFACE

Mercury lamps were used to photolyse  $(\text{CH}_3)_2\text{S}_2$ ,  $(\text{CH}_3)_2\text{S}$ ,  $\text{CH}_3\text{SH}$ ,  $\text{CD}_3\text{SH}$  and  $\text{CH}_3\text{SD}$  at 77K and 17K. The photolyses were followed by E.S.R. and infrared spectroscopy. Some samples consisted of the pure solid while others were trapped in an argon isolation matrix.

The infrared spectrum of  $\text{CD}_3\text{SH}$  is presented and analysed.

## CONTENTS

Introduction	1
Experimental	14
Vibrational Spectrum of Methanethiol-d <sub>3</sub>	23
Photolysis Results	46
Discussion	58
Bibliography	91

## INTRODUCTION

This project commenced as an attempt to isolate thioformaldehyde ( $\text{H}_2\text{CS}$ ) molecules and to identify them by recording their fundamentals in the infrared. Thioformaldehyde is known to trimerize into a ring compound under normal conditions and for this reason the monomer was unknown at the commencement of this work. It has recently been detected by two sets of workers. Callear and Dickson(1) observed the electronic spectrum in the flash photolysis of methyl disulphide, methyl sulphide, methanethiol and ethanethiol. Its microwave spectrum was obtained by Johnson and Powell(2) who reacted carbon disulphide with the products of a radio-frequency discharge in methane. Its infrared spectrum however is still unknown.

The approach used in the present work was to isolate molecules of methanethiol ( $\text{CH}_3\text{SH}$ ), dimethyl disulphide ( $\text{CH}_3\text{SSCH}_3$ ), or dimethyl sulphide ( $\text{CH}_3\text{SCH}_3$ ) in an argon matrix at 17 K and to photolyse them with ultraviolet light in order to break the molecules into smaller fragments. A short review(3) on inert gas matrix techniques has recently been published and a more comprehensive work is available(4). The reasons for selecting the three compounds used are shown below.

## Methanethiol

Methanethiol is known to absorb in the ultraviolet (5). It is generally agreed that when photolysed with various light sources the major primary photolytic process is S-H cleavage(1, 6-12) although there is wide disagreement concerning the amounts of various products.



It was anticipated that these two fragments produced in the matrix cage may undergo a rapid disproportionation (a radical-radical reaction which should have zero activation energy).



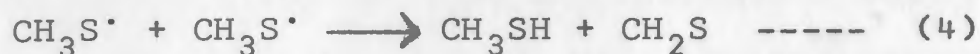
and hence thioformaldehyde monomer may be isolated in the matrix and readily observed.

## Methyl disulphide

When this compound absorbs in the ultraviolet(5) the most important primary photolytic step is known to be S-S cleavage(1, 13-18).



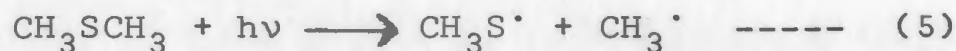
Again a disproportionation reaction may occur between the two thiyl radicals trapped in the cage



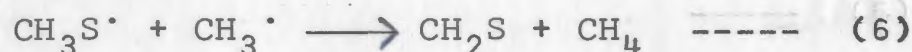
and thioformaldehyde may be observed.

### Methyl sulphide

The only primary photolytic step reported is C-S cleavage(1, 18-20) when this compound absorbs in the ultraviolet(5).



A radical-radical disproportionation in the cage would again yield thioformaldehyde monomer.



### Extension of the project to include E. S. R. spectra

In anticipation of the results chapter it can be indicated that many absorptions were obtained in the above infrared experiments. They were mainly weak and offered little opportunity for varying conditions to alter intensity ratios, and hence assign them to different species. There were however, many more absorptions

than could be accounted for by the mechanisms outlined above.

Accordingly a series of E.S.R. experiments was undertaken to provide some insight into the full decomposition mechanisms involved. The mechanisms were expected to be a free radical processes and it was hoped that the E.S.R. spectra recorded during the photolysis of the compounds would detect at least some of the radicals which were precursors to the species observed in the infrared. Since E.S.R. is much more sensitive than infrared it was possible that radicals present in low concentrations as intermediaries would be observed in the former but not in the latter.

## Vibrational Spectra

### Normal modes of vibration

A molecule containing  $n$  atoms will require  $3n$  cartesian coordinates to describe it and will accordingly have  $3n$  degrees of freedom. Six (five for a linear molecule) of these will be non-genuine vibrations, being classified as three translations and three (two for a linear molecule) rotations. The remaining  $3n-6$  ( $3n-5$  for a linear molecule) degrees of freedom will be genuine

vibrations involving bond stretching and bending. In some cases it is possible to identify a particular vibrational mode with the stretching of a specific bond or the bending of a specific angle. In the case of molecules containing larger numbers of atoms however, many of the vibrations may involve changes in several of the bond lengths and angles and the identification of the vibration with a specific bond or angle is then very approximate.

#### Interaction of vibrations with electromagnetic radiation

The vibrations of molecules have quantized energy levels (given by the quantum numbers  $v_i$ ) and the differences in the energy levels are of the same magnitude as the energy of infrared radiation. A vibration which causes a change in the dipole moment of the molecule can interact with infrared radiation of appropriate energy by absorption of a photon, thus elevating the vibration to a higher energy level. Infrared absorptions can be observed for samples in the gas, liquid or solid phases, with the frequencies observed in the condensed phases usually being slightly lower than the gas phase frequencies for the larger energy absorptions, and slightly higher for the smaller energy absorptions. Vibrations affecting parts of a molecule which are hydrogen bonded

in condensed phases result in much more intense absorptions in those phases. This arises because of the hydrogen bonding causing an increased dipole moment which can lead to larger changes during the vibration.

It is also possible for higher energy electromagnetic radiation to interact with vibrations if those vibrations change the polarizability of the molecule. If the frequency of the radiation is  $\nu$  and the energy change for the vibrational transition is  $\Delta E$ , then two new frequencies ( $\nu'$ ) will be observed.

$$\nu' = \nu \pm \frac{\Delta E}{h} \text{ -----(i)}$$

This is the basis of Raman spectroscopy which is complementary to infrared spectroscopy in that vibrations which are weak in the infrared tend to be strong in the Raman and vice-versa. Raman spectroscopy was of minor importance in the present work so it will not be dealt with further at this point.

### Vibration-rotation spectra

The rotational energy of a molecule is also quantized with quantum numbers  $J$  (referring to the total angular momentum) and  $K$  (referring to the angular momentum along a unique axis). The difference between rotational energy

levels is about one hundredth that between vibrational energy levels and a pure rotational transition is observed in the microwave region of the electromagnetic spectrum.

When a molecule is in the gas phase it will be simultaneously rotating and vibrating and transitions will frequently occur which will involve changes in both rotational and vibrational energy. Thus the vibrational spectrum of a molecule in the gas phase becomes a vibration-rotation spectrum with each vibrational transition showing many closely spaced lines corresponding to different changes in the rotational energy which can accompany that vibrational transition.

The selection rules which show the allowed changes in  $v_i$ ,  $J$ , and  $K$  depend upon the symmetry of the molecule and upon the particular vibration being considered. An asymmetric rotor (one with three different principal moments of inertia  $I_A < I_B < I_C$ ) will have three different sets of selection rules according to whether the vibration causes a change in dipole moment along the A, B or C axis. Accordingly the three types of vibration will show different sets of absorption lines which are classified as type A, B or C bands. Some transitions will concern a vibration which causes a change in the

component of the dipole moment along two or all three of these principal axes. In this case the infrared band will be a superposition of two or all three of the A, B and C types and is referred to as a hybrid band.

### E.S.R. Spectroscopy

This spectroscopic technique is dependent upon the intrinsic angular momentum of an electron (its 'spin') giving rise to different energy levels according to its orientation in an applied magnetic field. When exposed to radiation of suitable energy the spin can be reoriented by exchange of energy and hence the name 'Electron Spin Resonance'. The electrons concerned in E.S.R. experiments are unpaired electrons contained in various chemical species and their total angular momentum will therefore normally contain an orbital contribution resulting from spin-orbit coupling. This contribution may be large or small (according to the nature of the electronic orbital) and will cause a corresponding shift in the position of the absorption.

### The basis of E.S.R.

A species which contains an unpaired electron will have a net electron spin and hence a net electronic

magnetic moment ( $\mu$ ) which will interact with an applied magnetic field (H)

$$\text{Interaction} = \mu H \text{ ----- (ii)}$$

According to the laws of quantum mechanics this magnetic moment will be quantized in the reference direction (in this case the direction of H) which is designated as the z-axis. Hence

$$\text{Interaction} = \mu_z H_z \text{ ----- (iii)}$$

For a point charge the magnitude of the magnetic moment can be shown to be

$$\mu_z = \frac{e}{2mc} \cdot S_z = \pm \frac{e\hbar}{4mc} \text{ ----- (iv)}$$

Where  $e$  and  $m$  are the electronic charge and mass respectively, and  $c$  is the velocity of light.  $S_z$  is the angular momentum of the electron along the z-axis which can take the values  $\pm \frac{1}{2}\hbar$  for a single electron. Upon removing the fiction that electrons are point charges, equation (iv) is modified by the inclusion of a numerical g-factor called the Landé splitting factor.

$$\mu_z = \pm \frac{ge\hbar}{4mc} = \mp \frac{1}{2}g\beta \text{ ----- (v)}$$

where the expression  $-\frac{e\hbar}{2mc}$  is conveniently replaced by the constant  $\beta$  called the Bohr magneton. Substitution of  $\mu_z$  from (v) into (iii) provides

$$\text{Interaction} = \pm \frac{1}{2}g\beta H_z \text{ ----- (vi)}$$

Therefore the interaction of a single electron spin with an applied magnetic field allows two energy levels  $+\frac{1}{2}g\beta H_z$  and  $-\frac{1}{2}g\beta H_z$  corresponding to the two quantized values of the magnetic moment of the electron. If now an electron is exposed to radiation whose energy is equal to the difference between the two levels ( $g\beta H_z$ ), energy can be exchanged between the two systems resulting in a net absorption by the electron. This will occur with radiation of frequency  $\nu$  such that

$$g\beta H_z = h\nu \text{ ----- (vii)}$$

### Experimental considerations

Equation (vii) shows that theoretically radiation of any frequency can be used if the magnetic field has the appropriate magnitude. For practical reasons however microwave radiation is normally used. For radiation in the X band (8.5 to 9.6 GHz) a field of a few hundred millitesla is required. Again practical experience shows that it is more convenient to keep the frequency fixed and vary the field rather than the reverse. Finally the modulation method used in scanning the field leads to a first derivative of the absorption

curve and E.S.R. spectra are conventionally recorded and presented in this manner.

### Positions of Absorptions

The position of the absorption in E.S.R. spectroscopy is determined by the ratio of frequency to field or more conveniently by the g-factor. The majority of free radical E.S.R. absorptions occur very close to the g-factor of a free electron (2.0023). Large changes sometimes occur when an electron is closely associated with a particular atom in an orbital other than an s orbital. In such a case the angular momentum of the electron contains a large orbital contribution. g-factors can be calculated theoretically from the Landé expression

$$g = \frac{3}{2} + \frac{S(S+1) - L(L+1)}{2J(J+1)} \text{ ----- (viii)}$$

where S, L and J are quantum numbers for spin, orbital and total angular momentum.

### Anisotropic signals

If the field is applied along different axes of a species containing an unpaired electron, then the orbital contribution to the g-factor will result from the orbital motion induced about the different axes. This means that

different orbitals will be involved for different orientations of the species in the field. If these orbitals are not degenerate the orbital contribution to the g-factor will differ and hence three different g-factors will be observed (g is then written as a tensor). For a single crystal having preferred orientation of the species, different orientations of the crystal in the field will show the different g values. With polycrystalline, powdered or glassy samples however, the paramagnetic species will be randomly oriented and the same combination of g values will be observed in the same anisotropic signal regardless of orientation of the sample.

### Hyperfine interaction with nuclei

If the unpaired electron spends some of its time in the neighbourhood of a nucleus with non-zero spin then coupling will occur. Two types of coupling can occur; (a) due to an isotropic (contact) interaction and (b) due to an anisotropic (dipolar) interaction. The former is of most importance in the present work and will be dealt with briefly here. The isotropic interaction will produce extra energy levels which will allow more transitions and hence the resonance line of the electron will be split into a multiplet. A nucleus of spin I

will produce  $(2I + 1)$  lines of equal intensity. The magnitude of the splitting depends mainly on the electron density at the nucleus. With  $n$  equivalent nuclei each of spin  $I$ , the resonance line will be split into  $(2nI + 1)$  components. These components will all be split by the same amount, but their intensities will not be equal.

## EXPERIMENTAL

### Chemicals

The  $\text{CH}_3\text{SH}$ ,  $\text{CH}_3\text{SSCH}_3$  and  $\text{CH}_3\text{SCH}_3$  were supplied by the Eastman Kodak Company and were subjected to several freeze-pump-thaw cycles and several distillations in vacuo before use.

$\text{CH}_3\text{SD}$  was prepared from the  $\text{CH}_3\text{SH}$  by two exchanges with  $\text{D}_2\text{O}$  in a sealed tube. It was found to be better than 90% deuterated by N.M.R. spectroscopy.  $\text{CD}_3\text{SH}$  was prepared from  $\text{CD}_3\text{I}$ . Thiourea and  $\text{CD}_3\text{I}$  were sealed in a strong tube and maintained at 373 K for at least twenty-four hours. The thiuronium salt produced in the tube was then refluxed with 10% aqueous sodium hydroxide. The vapours emerging from the top of the reflux condenser were passed through medium strength sulphuric acid (to remove ammonia) and then water. The product was collected in a cold trap placed in an acetone slush bath. A slow stream of nitrogen was passed through the apparatus to exclude atmospheric gases and to help to carry over the product. The cold trap was then connected to a vacuum line and evacuated. The product was distilled into a tube containing phosphorus pentoxide and left to stand at 273 K for one hour. It could then be distilled off

and stored at 77 K in vacuo until required. This experimental procedure was perfected using  $\text{CH}_3\text{I}$  initially, and the purity of the  $\text{CH}_3\text{SH}$  checked by infrared and N.M.R. spectra. Neither spectrum showed any impurity compared with reported infrared(21) and N.M.R.(22) spectra. The infrared spectrum of  $\text{CD}_3\text{SH}$  has not been reported. It is presented and analyzed in the next chapter of this dissertation.

Methanethiol has two solid phases with a transition temperature at 137.6 K which is 12.6 K below its melting point. Rapid cooling of pure methanethiol by plunging the sample into liquid nitrogen invariably produces the high temperature form(23) which was normally used in the E.S.R. experiments. A few runs were performed with the low temperature phase which can be obtained by maintaining the sample just below the transition temperature for at least five hours(24). This was done by preparing a slush bath from a mixture of n-pentane and 2-methylbutane. The temperature of the slush bath was determined to be 136 K by a constantan-chromel thermocouple with a micro-voltmeter.

The argon used in the matrix isolation experiments was Matheson prepurified grade with nominal 99.998% purity.

## N.M.R. Spectra

The spectra were recorded at 60 MHz on a Varian A60 instrument. The samples were in 30% solution in  $\text{CDCl}_3$  with tetramethylsilane as internal reference, and the spectra were recorded at 265K.

## Infrared Spectra

### Spectrometers

For the routine infrared spectra the samples were contained in a gas cell with sodium chloride windows. Perkin Elmer 237B and 457 Grating Infrared Spectrophotometers were used to record the spectra in the region  $4000 \text{ cm}^{-1} - 600 \text{ cm}^{-1}$ .

The gas phase spectra for the  $\text{CD}_3\text{SH}$  analysis were recorded on a Perkin Elmer 225 double-beam, double-monochromator (KBr prism and two gratings) spectrometer, with the sample at  $34.0 \text{ kNm}^{-2}$  pressure in a gas cell equipped with potassium bromide windows. The region scanned was  $5000 \text{ cm}^{-1} - 350 \text{ cm}^{-1}$  using a slit programme of 2.5 which gave a spectral slit width of  $0.35 \text{ cm}^{-1}$  at  $700 \text{ cm}^{-1}$  and  $0.3 \text{ cm}^{-1}$  at  $2600 \text{ cm}^{-1}$  (the regions where rotational analysis was carried out).

The spectra for all the photolysis experiments were

recorded on the Perkin Elmer 225 instrument between  $4000\text{ cm}^{-1}$  and  $350\text{ cm}^{-1}$  at 17 K. The slit programme was 3.5 or 4 in these experiments giving a spectral slit width of  $0.4\text{ cm}^{-1}$  —  $0.9\text{ cm}^{-1}$  for most of the region scanned.

For all the spectra recorded on the 225 spectrometer the sample compartment was flushed with dry air from the recirculating purging unit of the instrument. During the matrix experiments a plastic cover was constructed around the cryostat since the latter prevented the normal sample compartment cover from being fitted.

#### The matrix experiments

The sample was frozen on a caesium iodide window mounted on the cold finger of an AC2L Cryo-tip system supplied by Air Products and Chemicals Limited. The system enabled the cold finger to be rotated without deterioration of vacuum. Hence the window could be turned to three different positions: (i) to allow deposition of the sample from a glass tube leading from a vacuum manifold, (ii) to expose the window to the photolysis lamp, (iii) to enable an infrared scan of the sample on the window to be taken. The Cryo-tip refrigerator used liquid nitrogen to cool hydrogen gas below its inversion temperature. The hydrogen was then

expanded through a small orifice to produce further cooling by the Joule-Thompson effect. In this way the boiling point of hydrogen (20.4K) could be reached. By pumping on the gas emerging from the orifice the temperature was further reduced to 17K.

The samples in argon were generally at a matrix to monomer ratio of 250:1 and were prepared in a five-litre bulb attached to the vacuum line. They were prepared the day before the experiment was run to allow thorough mixing overnight. The sample was deposited on the window by leading it through the vacuum line at approximately 40 micromoles of sulphur compound during a two hour period.

For the experiments on methanethiol which were done without an isolation matrix, sufficient sample was deposited in thirty minutes. This deposition was carried out at 77K by stopping the flow of hydrogen when the normal boiling point of liquid nitrogen was reached. The hydrogen flow was then recommenced to carry out the remainder of the experiment at 17K.

Both low pressure and high pressure mercury lamps were used for photolysis in the infrared experiments. The low pressure lamp was constructed to Dr. Ogilvie's design and operated at 7.5 watts. At this power the

lamp was a little above room temperature and the mercury vapor pressure correspondingly low. Radiation would be almost exclusively the 253.7-nm resonance line. The high pressure source was a Philips HPK-125 lamp operating at 125 watts and providing a continuum of wavelengths extending to higher energies.

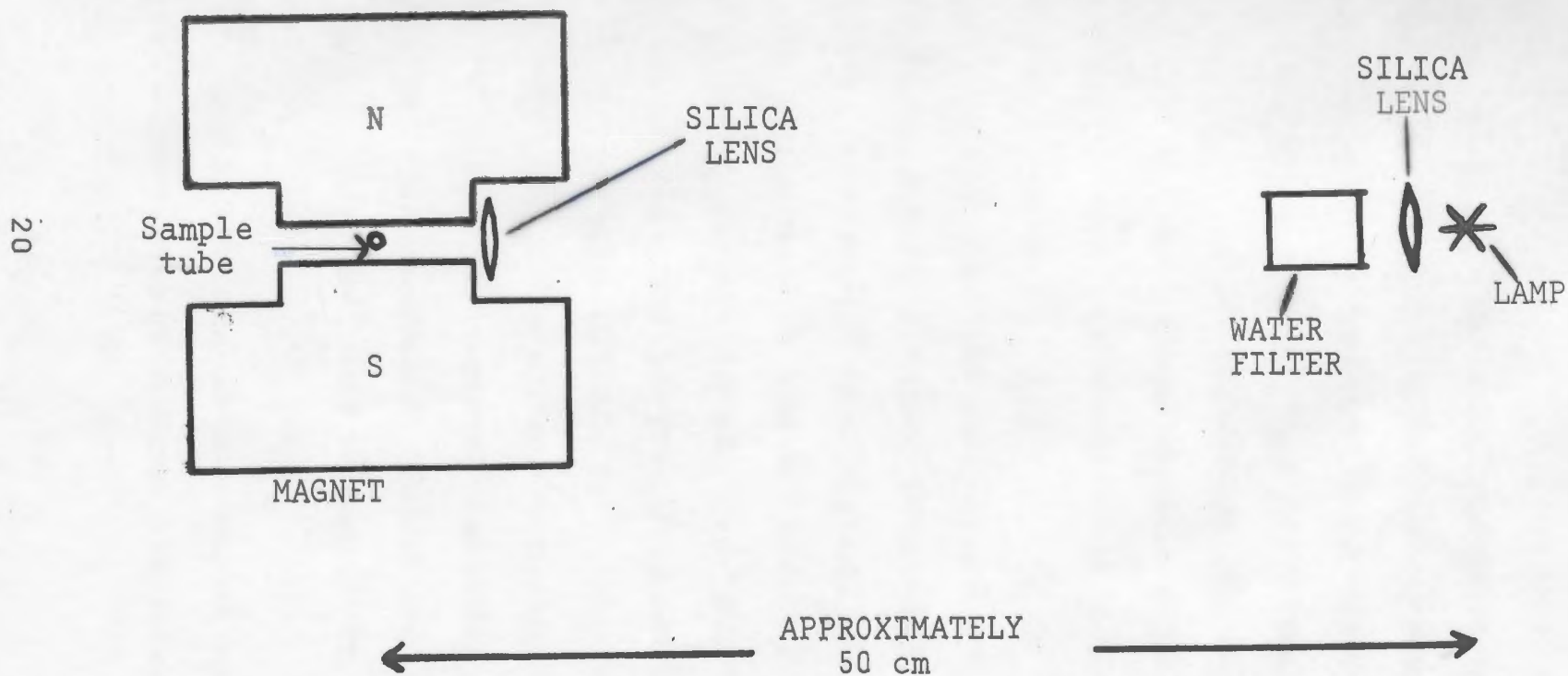
### Raman Spectra

These were recorded on a Coderg Raman Laser type PHO spectrometer. The laser was a Coherent Radiation model 52 Argon/Krypton mixed gas ion laser and the 488-nm and 514.5-nm Argon ion emission lines were used. A half-wave plate was used to generate the polarization data.

### E.S.R. Spectra

These were used to follow the photolysis of methanethiol, methyl disulphide and methyl sulphide. The compounds were vacuum distilled into 5-mm silica sample tubes and sealed with a ground glass tap while frozen with liquid nitrogen. The sample tube was placed in a liquid nitrogen quartz dewar insert which was placed in the cavity of the E.S.R. instrument. Photolysis with an Osram HBO 500 W/2 500 watt high pressure mercury lamp was performed in situ while scans

Figure 1. Arrangement for E.S.R. photolysis experiments.



were being taken, the experimental arrangement being shown in figure 1.

The spectrometer was a JEOL Jes ME 3X instrument operating in X-band with 100 kHz. modulation frequency; the magnet had a diameter of twelve inches. Spectra were recorded as the first derivative. The field was calibrated with a  $Mn^{2+}$  sample in magnesium oxide and this spectrum was in turn calibrated with an N.M.R. gaussmeter. Frequencies were measured using a Hewlett-Packard X532B frequency meter.

Non-linearity and drift of the field led to larger errors in the g-factors and splittings than might be expected. To avoid saturation of the signal, all spectra were recorded at the low power of one milliwatt and a check was made that the signals did not vary with a four-fold increase or decrease of the power. Modulation widths were between 0.1 mT and 0.5 mT.

To obtain a crude annealing effect the sample tube was lifted out of the dewar for several seconds, wiped with a tissue moistened with methanol to remove condensed water vapour and carbon dioxide, and replaced in the dewar.

To rotate the sample in some methanethiol experiments, a paper scale was fastened around the dewar and

and read opposite a fixed reference point. The rotation of the dewar (containing the sample) was normally made in  $22.5^\circ$  steps thus requiring sixteen steps for a full turn.

Early experiments were performed using silica tubing supplied by the General Electric Company. However this tubing was found to give rise to a strong signal near  $g=2$ , so a tube supplied by Wilmad was used for the later experiments.

## VIBRATIONAL SPECTRUM OF METHANETHIOL - d<sub>3</sub>

### Vibrational Assignment

The infrared spectra of CH<sub>3</sub>SH and CH<sub>3</sub>SD have been recently investigated(21). That of CD<sub>3</sub>SH has not been reported; it is now presented in figures 2-4. Several investigations(25-27) of the microwave spectrum of methanethiol have been carried out, the latest of these by Kojima(25) showing the molecule to have C<sub>s</sub> symmetry with the geometry illustrated in figure 5.

Such a molecule is expected to have its twelve normal modes divided into eight symmetric (A') vibrations and four antisymmetric (A'') vibrations with all of them active in both the Raman and the infrared(28). Four of the symmetric vibrations should be close to the four antisymmetric vibrations, since if C-S-H were linear (prolate symmetric top molecule with C<sub>3v</sub> symmetry) they would coincide and form four doubly degenerate vibrations. The splitting is expected to be slight for the methyl group, but it should be large for the deformation vibrations of the (D<sub>3</sub>)-C-S-H chain. This is observed in table 1.

The A'' vibrations will produce a changing dipole

Figure 2a: Infrared spectrum of  $\text{CD}_3\text{SH}$  in the gas phase.

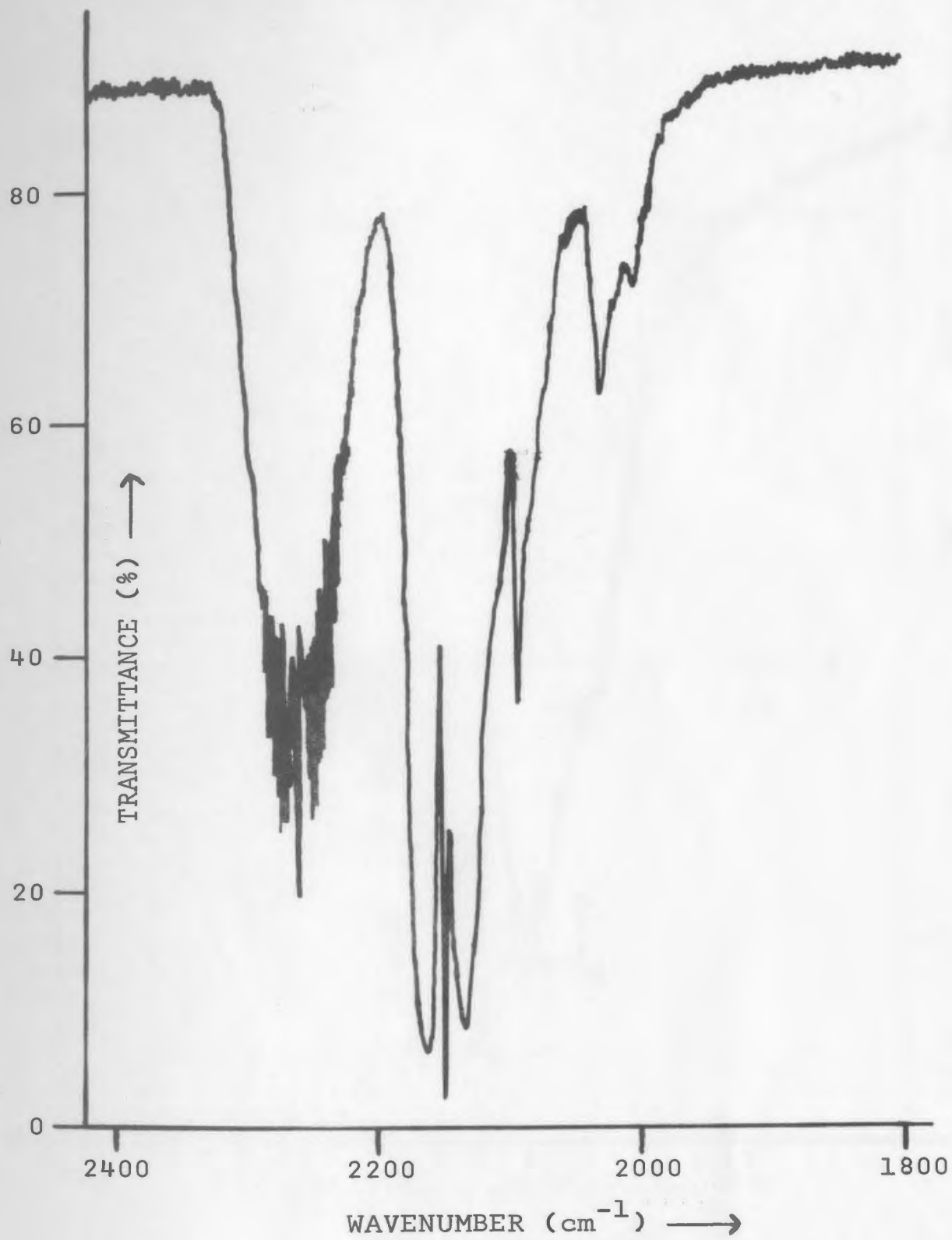


Figure 2b: Infrared spectrum of  $\text{CD}_3\text{SH}$  in the gas phase

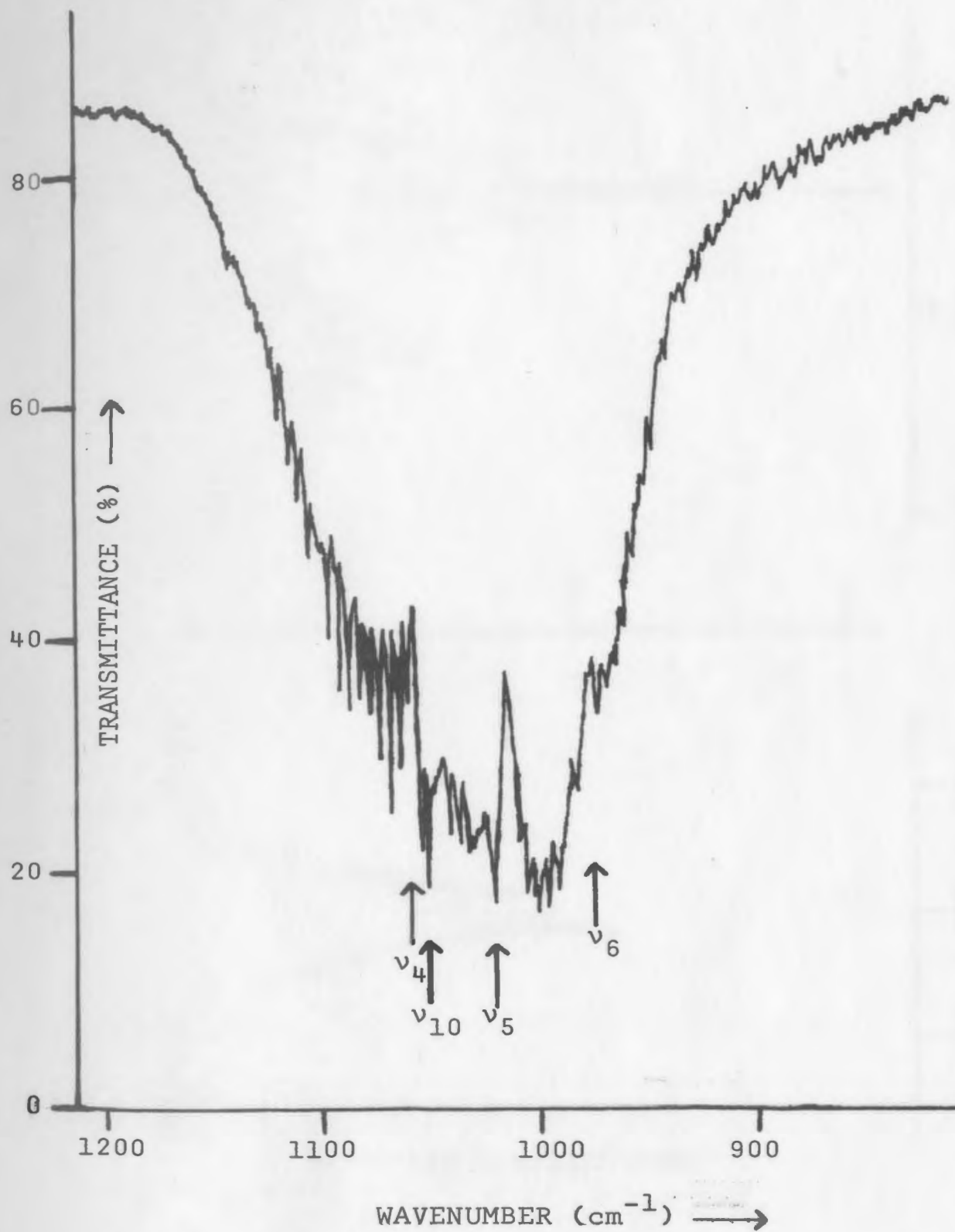


Figure 2c: Infrared spectrum of  $\text{CD}_3\text{SH}$  in the gas phase.

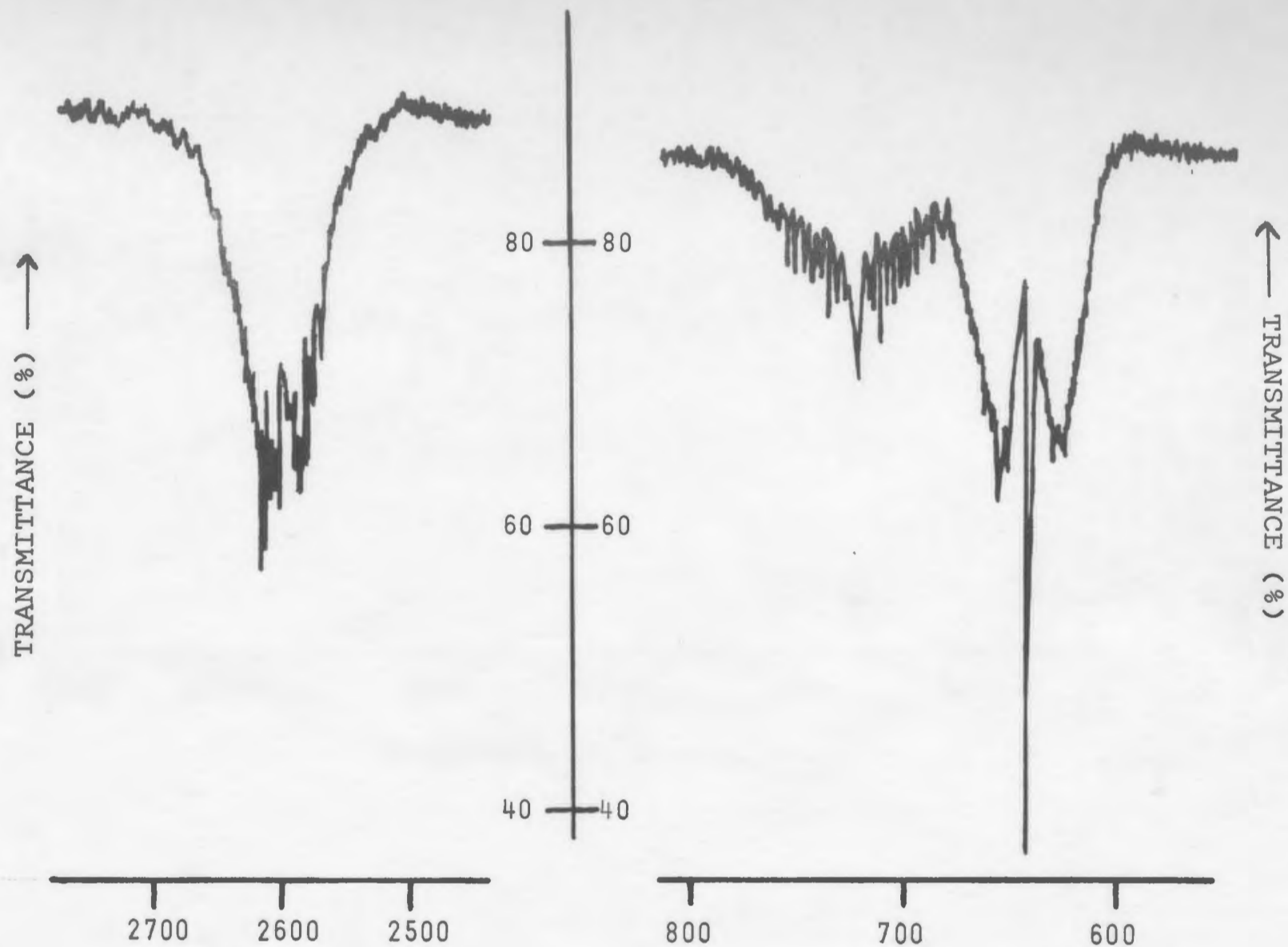


Figure 2d: Infrared spectrum of  $\text{CD}_3\text{SH}$  in the gas phase.

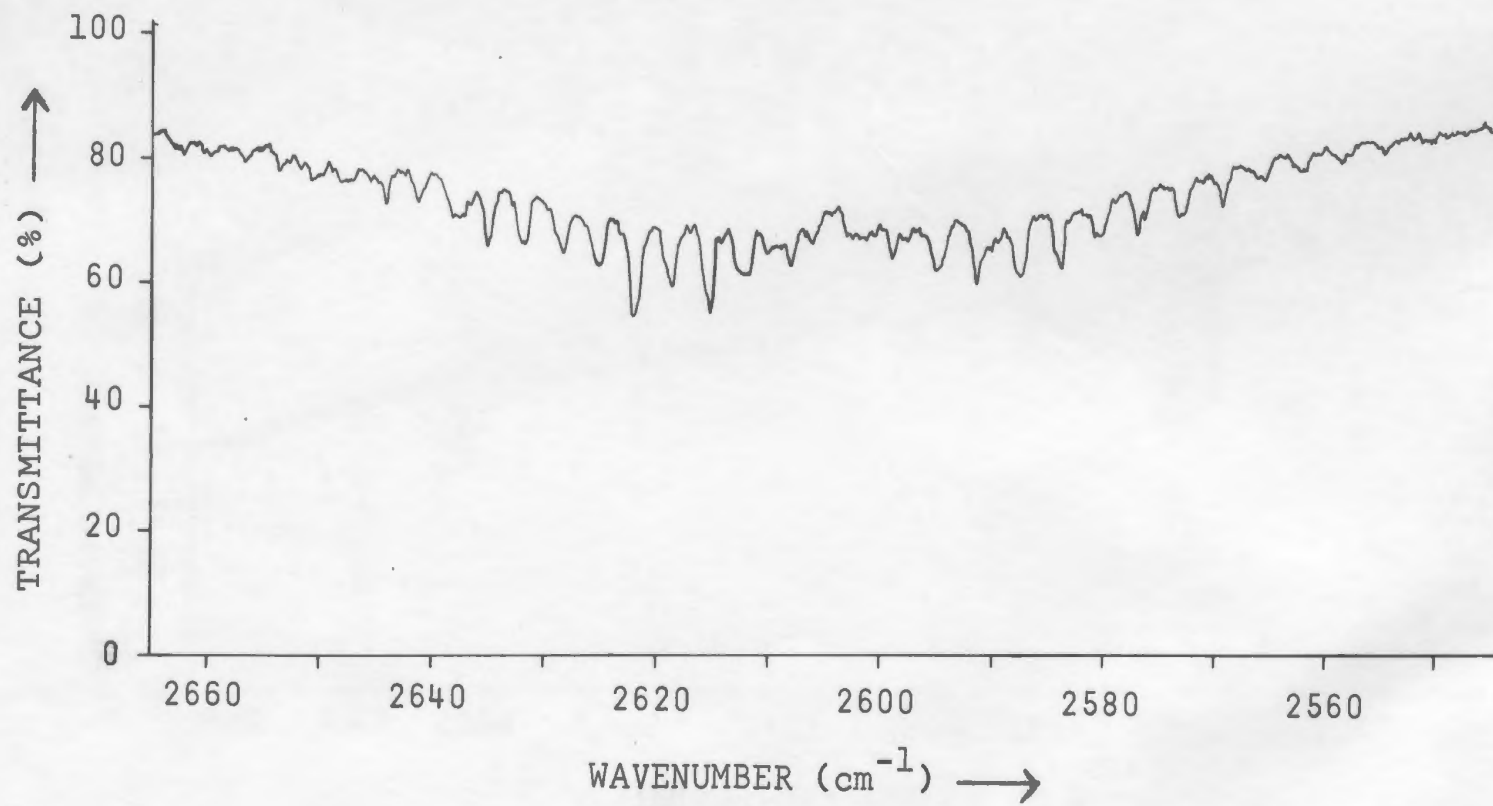


Figure 3: Infrared spectrum of  $\text{CD}_3\text{SH}$  in an argon matrix.

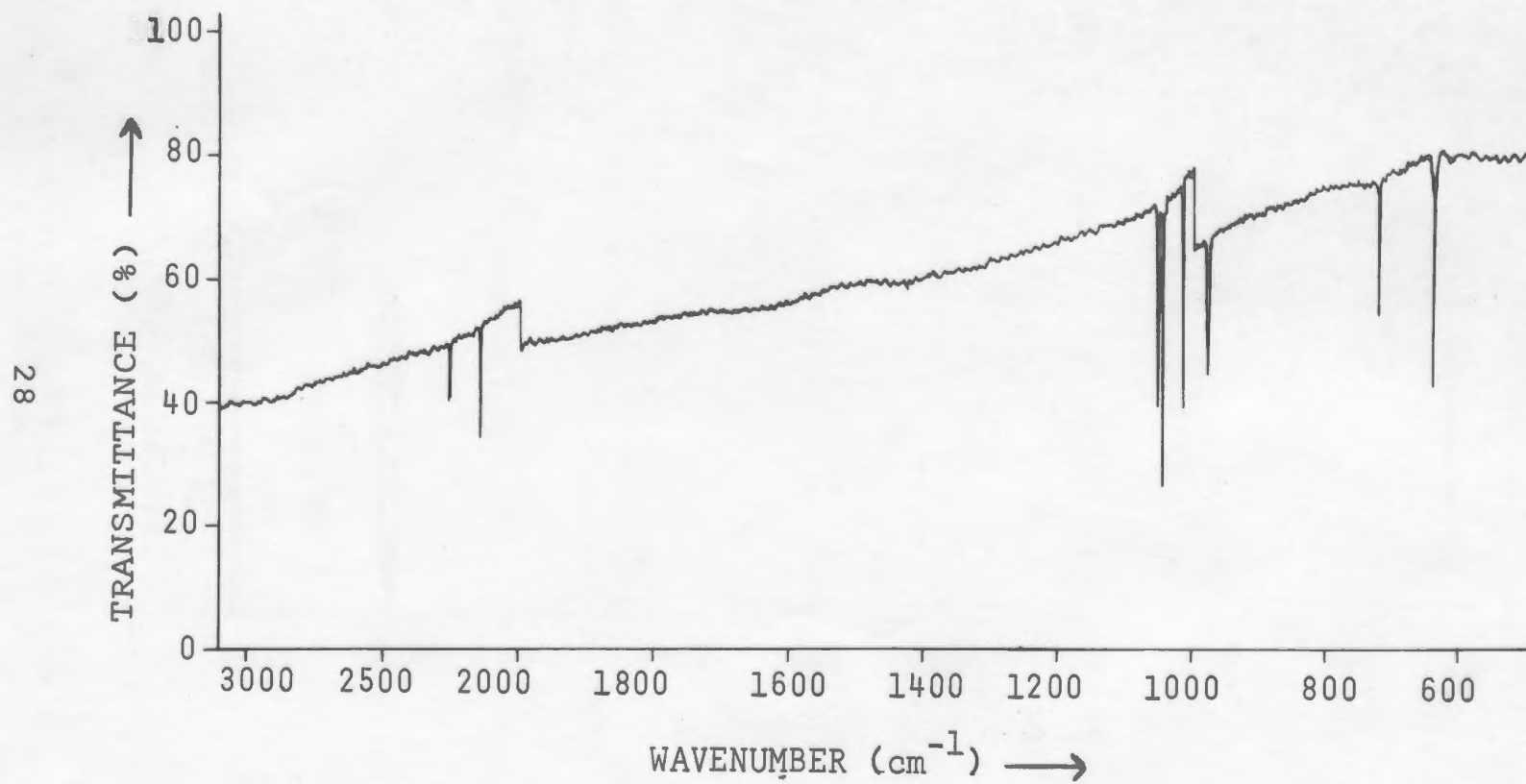


Figure 4: Infrared spectrum of solid  $\text{CD}_3\text{SH}$ .

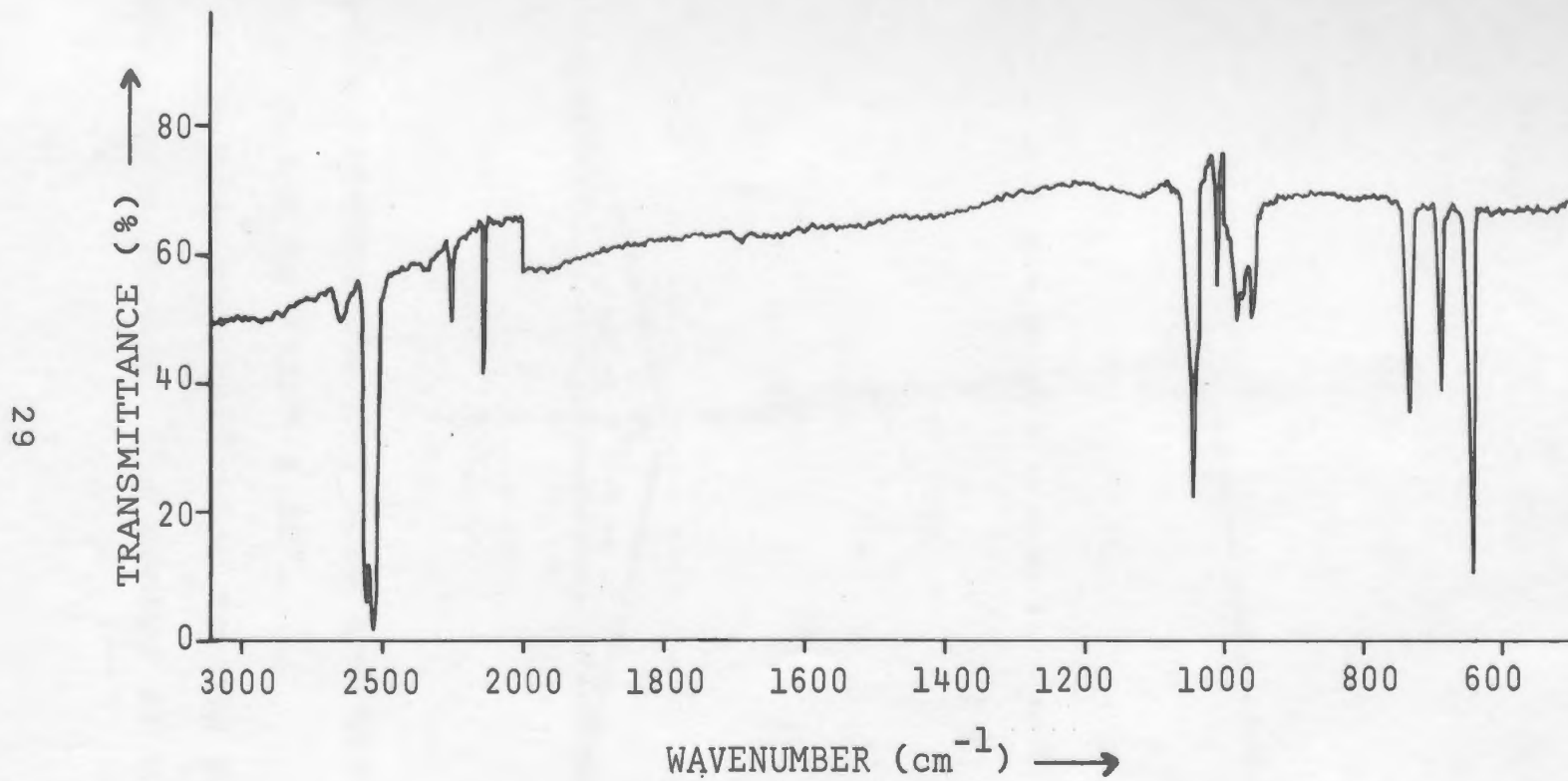


Figure 5: Structure of the methanethiol molecule  
(After Kojima).

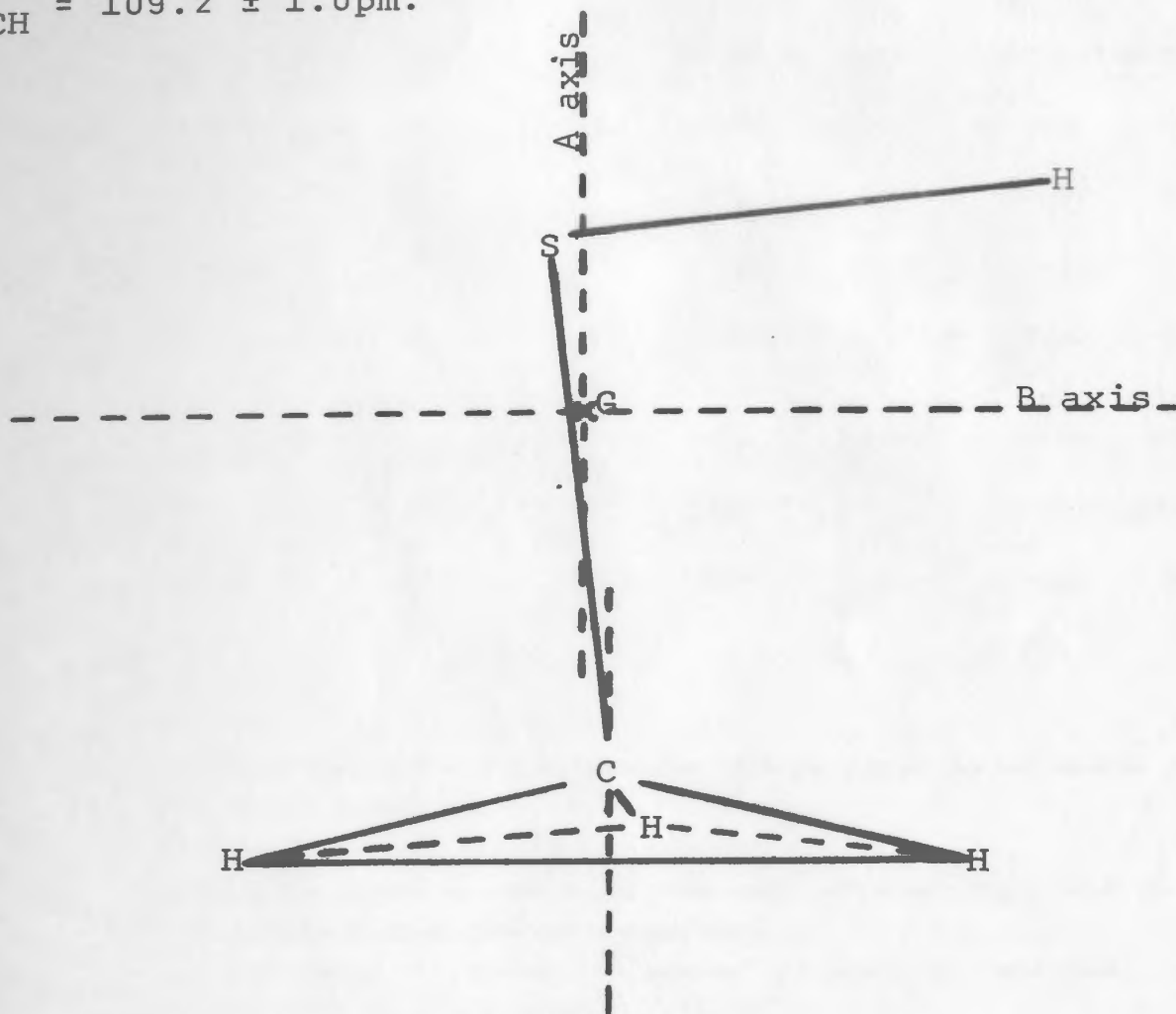
$$d_{SH} = 133.5 \pm 1.0 \text{ pm.}$$

$$d_{CS} = 181.9 \pm 0.5 \text{ pm.}$$

$$d_{CH} = 109.2 \pm 1.0 \text{ pm.}$$

$$\angle CSH = 96^\circ 30' \pm 30'.$$

$$\angle HCH = 109^\circ 45' \pm 30'.$$



The angle between the C-S bond and the symmetry axis of the methyl group is  $2^\circ 10' \pm 30'$ .

The C axis lies perpendicular to the plane of the molecule and passes through the centre of mass G.

Table 1. Observed and calculated infrared and Raman vibrational wavenumbers ( $\text{cm}^{-1}$ ) for  $\text{CD}_3\text{SH}$ .

Vibration	Approximate description	Type of band	I.R.	I.R. in	I.R.	Raman	Calculated	
			Vapour <sup>†</sup>	Argon <sup>†</sup>	Solid <sup>†</sup>	liquid <sup>†</sup>	S.V.F.F.	M.V.F.F.
A'	$\nu_1$ C-D antisym. stretch	B	2257m	2254w	2250w	2253m,dp	2229	2229
			3015		3000	3001		
			3015		2999	3003		
	$\nu_2$ C-D sym. stretch	A	2149s	2146m	2135m	2137vs,p	2109	2109
			2948		2930	2933		
			2949		2933	2933		
	$\nu_3$ S-H stretch	B	2604w	-	2540*br,vs	2578vs,p	2614	2614
			2605		2543	2575		
			1893		1847	1871		
	$\nu_4$ $\text{CD}_3$ antisym. deformation	B	1060m	1055m	1045s	1050br,vw,dp	1049	1049
			1453		1434	1444		
			1453		1434	1440		
$\nu_5$ $\text{CD}_3$ symmetric deformation	A	1022m	1015m	1012	1014m,p	999	999	
		1332		1321	1323			
		1332		1321	1322			
$\nu_6$ $\text{CD}_3$ wag	B	979w	977m	972*br,m	976w,p?	743	912	
		1072		1070	1064			
		1007		1005	1000			
$\nu_7$ S-H bend	A	-	-	688m	687s,p	937	762	
		802		802	806			
		623		621	624			
$\nu_8$ C-S stretch	A	644m	643m	643s	649m,p	635	635	
		710		703	704			
		717		709	710			
A''	$\nu_9$ C-D antisym. stretch	C	2260s	2259w	2250w	2253m,dp	2229	2229
			3012		3000	3001		
			3011		2999	3003		
	$\nu_{10}$ $\text{CD}_3$ antisym. deformation	C	1052m	1046m	1045s	1050br,vw,dp	1049	1049
			1444		1434	1444		
			1444		1434	1440		
	$\nu_{11}$ $\text{CD}_3$ wag	C	726w	724m	733m	706m,dp	743	743
			956		955	964		
			963		970	967		
	$\nu_{12}$ Torsion	C				146w?		

In the above table a blank in the column indicates that the region was not scanned. A dash (-) indicates no detectable absorption.

\* Average of observed bands in high temperature phase.

† Frequencies listed in order  $\text{CD}_3\text{SH}$  (this work),  $\text{CH}_3\text{SH}$  and  $\text{CH}_3\text{SD}$  (Both due to May and Pace)

‡ Frequencies of  $\text{CD}_3\text{SH}$  from the present work.

vs = very strong; s = strong; m = medium; w = weak; vw = very weak; br = broad;

p = polarized; dp = depolarized.

Table 2. Gas phase overtone and combination bands of  $\text{CD}_3\text{SH}$  observed in the infrared

Tentative Assignments	Observed Wavenumber ( $\text{cm}^{-1}$ )	Calculated Wavenumber ( $\text{cm}^{-1}$ )
$2\nu_1$	4468	4514
$\nu_3 + \nu_6$	3576	3583
$\nu_1 + \nu_5$	3270	$\left\{ \begin{array}{l} 3279 \\ 3271^* \end{array} \right.$
$\nu_3 + \nu_7$		
$\nu_1 + \nu_{11}$	2975	$\left. \begin{array}{l} 2983 \\ 2986 \end{array} \right\}$
$2\nu_{10}$	2095	2104
$2\nu_5$	2020	$\left\{ \begin{array}{l} 2044 \\ 2039 \end{array} \right.$
$\nu_4 + \nu_6$		
$\nu_6 + \nu_{11}$	1696	1705
Impurity?	1400	

In all of the above assignments  $\nu_1$  can be replaced by  $\nu_9$ . Thus  $2\nu_1$  could be  $2\nu_9$  or  $\nu_1 + \nu_9$  etc.  $2\nu_{10}$  could be replaced by  $2\nu_4$  (see comments).

\*Calculated using the product rule wavenumber of  $667 \text{ cm}^{-1}$  for  $\nu_7$ .

moment along the C-axis and will therefore be assigned to type-C bands with small central Q branches.  $\nu_1$ ,  $\nu_3$ ,  $\nu_4$ , and  $\nu_6$  will produce changing dipole moments about  $2^\circ$  from the B-axis and will therefore be assigned to type-B bands with a minimum at the band origin. The other A' vibrations will produce a changing dipole moment about  $2^\circ$  from the A-axis and will therefore be assigned to type-A bands with a prominent Q branch and little or no fine structure.

#### 1. C-D stretching vibrations

The antisymmetrical C-D stretching vibrations  $\nu_1$ (A') and  $\nu_9$ (A'') are expected to be severely overlapped in the gas phase. The band system at approximately  $2260\text{ cm}^{-1}$  is assigned to these modes. May and Pace(21) in the spectra of methanethiol and Harvey and Wilson(29) in the spectra of methaneselenol have attempted to resolve these vibrations by arbitrarily assigning  $\nu_1$  to the most prominent minimum and  $\nu_9$  to the most intense subband. Such a procedure in the present case would place  $\nu_1$  at  $2257\text{ cm}^{-1}$  and  $\nu_9$  at  $2260\text{ cm}^{-1}$ , but these assignments must be dubious since a most prominent minimum will be present even if  $\nu_1$  and  $\nu_9$  are unresolvable. In the spectrum of  $\text{CD}_3\text{SH}$  in an argon matrix, two sharp absorption lines at  $2254\text{ cm}^{-1}$

and  $2259 \text{ cm}^{-1}$  can be assigned to the two components of the antisymmetric C-D stretch although the possibility that these two lines arise from matrix effects cannot be excluded.

The spectrum of solid  $\text{CD}_3\text{SH}$  shows a single broader absorption at  $2250 \text{ cm}^{-1}$  with no evidence for splitting of the components. A single depolarized Raman line appears at  $2253 \text{ cm}^{-1}$ .

The type-A band with a sharp Q-peak at  $2149 \text{ cm}^{-1}$  is identified with the symmetric C-D stretch  $\nu_2$  ( $A'$ ).

## 2. S-H stretching vibration

This  $\nu_3$  ( $A'$ ) vibration shows a type-B envelope with resolved fine structure and band minimum at  $2604 \text{ cm}^{-1}$ . There is no detectable absorption in the matrix isolation experiments but in the spectra of solid  $\text{CD}_3\text{SH}$  this vibration is very intense (due to the hydrogen bonding) with pronounced crystal splitting.

## 3. Methyl deformation

The two components of the antisymmetrical deformation are strongly overlapped. Following the somewhat arbitrary procedure used with the other internal vibrations of the methyl group,  $\nu_4$  ( $A'$ ) would be assigned to the band

minimum at  $1060 \text{ cm}^{-1}$  and  $\nu_{10}$  ( $A''$ ) to the most prominent Q branch at  $1052 \text{ cm}^{-1}$ . The matrix experiments show two sharp lines at  $1055 \text{ cm}^{-1}$  and  $1046 \text{ cm}^{-1}$ . Again no splitting of the components can be detected in the solid or Raman.

The type-A band with prominent Q branch at  $1022 \text{ cm}^{-1}$  is assigned to the symmetric deformation  $\nu_5$  ( $A'$ ). This vibration has some overlap with the antisymmetrical methyl deformations and with the  $A'$  methyl wag.

#### Methyl wagging and S-H bending vibrations

The S-H bend and the  $A'$  methyl wag are of the same symmetry and both involve deformation of the  $(D_3)-C-S-H$  chain. Accordingly they will be expected to interact and their descriptions as involving only S-H and methyl respectively must be very approximate. Such an interaction has been found in the methyl alcohols(30),  $\text{CH}_3\text{SH}$  and  $\text{CH}_3\text{SD}$ (21), and in the methaneselenols(29). The interaction causes the two vibrations to push apart and this repulsion is largest when the two vibrations would otherwise be close. Inspection of previous work on methanethiol(21) and methaneselenol(29) indicates that the repulsion will be very strong in  $\text{CD}_3\text{SH}$ . Since the  $A''$  methyl wag is of the wrong symmetry to interact with the S-H bend, the two components of the methyl wag will

be well separated. Hence  $\nu_6$  (A') is assigned to a well defined minimum at  $979 \text{ cm}^{-1}$  (origin of type-B band), and  $\nu_{11}$  (A'') is assigned to the type-C band with Q branch at  $726 \text{ cm}^{-1}$ . In the solid spectra  $\nu_6$  shows considerable crystal splitting. The depolarized Raman line at  $706 \text{ cm}^{-1}$  is assigned to  $\nu_{11}$  although agreement with the infrared wavenumbers is rather poor.

The S-H bend of  $\text{CH}_3\text{SH}$  appears as a very weak type-A band at  $802 \text{ cm}^{-1}$ . In the present case, the stronger repulsion with the A' methyl wag will be expected to push this vibration to a somewhat lower wavenumber. No absorption can be seen in this region of the gas phase or matrix spectra. Absorption in the solid however, would be expected to be more intense due to hydrogen bonding. Accordingly  $\nu_7$  (A') is assigned to a moderately intense line at  $688 \text{ cm}^{-1}$ . A strong polarized Raman line at  $687 \text{ cm}^{-1}$  supports this assignment.

Some of the difficulty in detecting this vibration in the infrared arises from the poor sensitivity of the spectrometer due to the strong absorption of atmospheric carbon dioxide in this region.

#### 5. C-S stretching vibration

The gas phase spectra show a type-A band envelope

with a very distinct Q branch at  $644 \text{ cm}^{-1}$  which is identified as  $\nu_8$  (A'). Good agreement is seen in the other spectra.

#### 6. Torsional vibration

The torsional oscillation of S-H is expected to lie below  $200 \text{ cm}^{-1}$ . This region was not scanned in the infrared but a line at  $146 \text{ cm}^{-1}$  appeared in the Raman. This may be the  $\nu_{12}$  (A'') vibration but it may possibly be a grating ghost. May and Pace(21) calculate  $\nu_{12}$  at  $191 \text{ cm}^{-1}$  for  $\text{CH}_3\text{SH}$  and at  $130 \text{ cm}^{-1}$  for  $\text{CH}_3\text{SD}$  but they did not observe this mode.

#### 7. Overtones and combinations

The features of the gas phase infrared spectra which are not attributed to fundamentals are listed with tentative assignments in table 2. All the bands are weak except those at  $2095 \text{ cm}^{-1}$  and  $2020 \text{ cm}^{-1}$  which are a little stronger, presumably due to Fermi resonance with the nearby  $\nu_2$  fundamental. Accordingly both of these bands are attributed to overtones of the same symmetry as  $\nu_2$  (A').  $2\nu_4$  (A'),  $2\nu_{10}$  (A'),  $(\nu_4 + \nu_5)$  (A'),  $(\nu_5 + \nu_{10})$  (A'') and  $(\nu_4 + \nu_{10})$  (A'') all have calculated wavenumbers close to the  $2095 \text{ cm}^{-1}$  absorption. From the symmetry considerations above, the last two of these are

rejected. Since the calculated wavenumber of an overtone is expected to be slightly higher than the observed wavenumber,  $2\nu_4$  or  $2\nu_{10}$  are preferred to  $(\nu_4 + \nu_5)$ . Considering the  $2020 \text{ cm}^{-1}$  band,  $(\nu_6 + \nu_{10})$  is rejected for the same symmetry reasons. No distinction can be made between  $\nu_4$  and  $\nu_{10}$  or between  $\nu_1$  and  $\nu_9$  in all the other assignments.

For the  $3270 \text{ cm}^{-1}$  overtone,  $(\nu_1 + \nu_5)$  is preferred to  $(\nu_3 + \nu_7)$  since the  $\nu_1$  and  $\nu_5$  bands are stronger than  $\nu_3$  and  $\nu_7$ . The weak absorption at  $1400 \text{ cm}^{-1}$  causes difficulty.  $2\nu_{11}$  (calculated wavenumber  $1452 \text{ cm}^{-1}$  shows a large discrepancy, the difference band  $(\nu_2 - \nu_{11})$  calculated at  $1423 \text{ cm}^{-1}$  is unlikely to be strong enough to be observed, and  $(\nu_7 + \nu_{11})$  at  $1406 \text{ cm}^{-1}$ , consisting of modes predominantly affecting opposite ends of the molecule, is an unlikely combination. Also despite a small amount of water affecting the spectrum in this region, the band appears to have a different shape from the other bands in the spectrum. It is therefore considered preferable to attribute this feature of the spectrum to some unknown species present as an impurity.

### Teller - Redlich Product Rule Calculation

The rule is given by Herzberg (reference 28, page

231) as

$$\frac{\omega_1^i}{\omega_1} \cdot \frac{\omega_2^i}{\omega_2} \dots \frac{\omega_f^i}{\omega_f} = \sqrt{\left(\frac{m_1}{m_1^i}\right)^\alpha \left(\frac{m_2}{m_2^i}\right)^\beta \dots \left(\frac{M}{M^i}\right)^t \left(\frac{I_A}{I_A^i}\right)^{\delta A} \left(\frac{I_B}{I_B^i}\right)^{\delta B} \left(\frac{I_C}{I_C^i}\right)^{\delta C}} \quad \text{---(IX)}$$

where all symbols with a superscript *i* refer to an isotopic molecule and symbols without the superscript refer to the regular molecule. The left hand side of the equation includes the zero-order frequencies ( $\omega$ ) for all vibrations of one symmetry type. The values of  $m_1$ ,  $m_2$  etc. are the total masses of the representative atoms of the various sets. The exponents  $\alpha$ ,  $\beta$  etc. are the number of vibrations (inclusive of non-genuine vibrations) each set contributes to the symmetry type considered.  $M$  is the total mass of the molecule;  $t$  is the number of translations of the symmetry type considered.  $I_A$ ,  $I_B$  and  $I_C$  are the moments of inertia about the A-, B- and C-axes (figure 5).  $\delta A$ ,  $\delta B$ ,  $\delta C$  are either one or zero depending on whether or not the rotation about the A, B, C axis is a non-genuine vibration of the symmetry species considered.

In the present work the rule was applied to the observed infrared gas phase frequencies of  $\text{CD}_3\text{SH}$  and  $\text{CH}_3\text{SH}$  as listed in table 1. Since no wavenumber was observed for  $\nu_7$  of  $\text{CD}_3\text{SH}$ , the rule was used to calculate

a value for this vibration at  $667 \text{ cm}^{-1}$ . An Olivetti-Underwood Program 101 was used for the numerical computation. In condensed phases hydrogen bonding would be expected to alter the position of this mode, probably to a higher wavenumber. The agreement of the product rule value with the Raman liquid ( $687 \text{ cm}^{-1}$ ) and infrared solid ( $688 \text{ cm}^{-1}$ ) values therefore appear to be acceptable.

### Normal Coordinate Analysis

Using the FG matrix approach of Wilson et al.(31, 32), the 'symmetrized force constants' listed by May and Pace(21) for  $\text{CH}_3\text{SH}$  and  $\text{CH}_3\text{SD}$  were assumed to be isotopically invariant and used to predict the vibrational wavenumbers of  $\text{CD}_3\text{SH}$ . The kinetic energy matrix was set up in internal coordinates ( $G_I$ ) from the G-matrix elements listed by Wilson, Decius and Cross(31). The elements were computed using the microwave results of Kojima(25) which are listed in figure 5 of the present work. The  $2^\circ$  deviation of the C-S bond from the three-fold axis of the methyl group was not included as it was found to be essentially negligible in the calculations of May and Pace(21). The transformation U-matrix and its transpose  $U'$  were set up from the symmetry

coordinates given by May and Pace(21). The G-matrix in symmetry coordinates ( $G_S$ ) was then obtained from the matrix multiplication

$$G_S = UG_I U' \quad \text{----- (X)}$$

The F-matrix in symmetry coordinates ( $F_S$ ) was set up directly using the symmetrized force constants of May and Pace(21) in a potential energy expression using symmetry coordinates. A further matrix multiplication  $G_S F_S$  enabled values of  $\lambda$  to be obtained from

$$|G_S F_S - \lambda| = 0 \quad \text{----- (XI)}$$

The values of  $\lambda$  obtained from this determinant were then used to calculate the wavenumbers  $\nu$  from

$$\lambda = 4\pi^2 \nu^2 \quad \text{----- (XII)}$$

The wavenumbers listed in the next to last column of table 1 were obtained using a simple valence force field (SVFF) expressed in the terms of the diagonal force constants only. The frequencies in the final column were obtained using a modified valence force field (MVFF) in which one interaction force constant coupling the A' methyl wagging vibration with the S-H bending vibration (A') was included. The torsional mode was not included in either of the calculations as it factorizes out readily because of its low frequency. All numerical calculations were carried out on a Wang

Calculator model 720B.

Except for the  $\nu_6$  and  $\nu_7$  modes the calculated wavenumbers show reasonable agreement with the observed values and provide good confirmation of the assignments which have been made. Without the interaction force constant  $K_{67}$ ,  $\nu_6$  is calculated at  $743 \text{ cm}^{-1}$  and  $\nu_7$  at  $937 \text{ cm}^{-1}$ . Reference to the observed wavenumbers of the methyl alcohols(30), the methaneselenols(29) and  $\text{CH}_3\text{SH}$ ,  $\text{CH}_3\text{SD}$ (21) as well as  $\nu_{11}$  of  $\text{CD}_3\text{SH}$  observed at  $726 \text{ cm}^{-1}$  in the present work, shows that these wavenumbers are in the regions where they would be expected to appear if no interactions occurred. With the one interaction term included in the calculation, the agreement with the observed values improves but is still rather poor.

### Rotational Analysis

In the vibration-rotation spectrum of  $\text{CD}_3\text{SH}$ , two bands were well separated from other bands and showed resolved fine structure thus offering opportunity for rotational analysis. The bands were  $\nu_3$  (type B) and  $\nu_{11}$  (type C). Figure 2d shows the  $\nu_3$  vibration on an expanded wavenumber scale and tables 3 and 4 show the combination sums and differences for the K-structure of the two bands. Since  $\text{CD}_3\text{SH}$  is very close to a

Table 3. Combination sums and differences ( $\text{cm}^{-1}$ ) for  $\text{CD}_3\text{SH } \nu_3$

K	$r_{\text{QK}}$	$\text{PQK}$	$r_{\text{QK}} + \text{PQK}$	$r_{\text{QK}} - \text{PQK}$	$r_{\text{QK}-1} - \text{PQK}+1$
1	2608.3				
2	2612.0	2599.2	5211.2	12.8	13.1
3	2615.5	2595.2	5210.7	20.3	20.3
4	2619.0	2591.7	5210.7	27.3	27.8
5	2622.3	2587.7	5210.0	34.6	35.0
6	2625.5	2584.0	5209.5	41.5	41.7
7	2628.6	2580.6	5209.2	48.0	48.2
8	2632.2	2577.3	5209.5	54.9	55.2
9	2635.4	2573.4	5208.8	62.0	62.7
10	2638.5	2569.5	5208.0	69.0	69.7
11	2641.5	2565.7	5207.2	75.8	76.3
12	2644.5	2562.2	5206.7	82.3	82.8

Table 4. Combination sums and differences ( $\text{cm}^{-1}$ ) for  $\text{CD}_3\text{SH } \nu_{11}$

K	$r_{\text{QK}}$	$\text{PQK}$	$r_{\text{QK}} + \text{PQK}$	$r_{\text{QK}} - \text{PQK}$	$r_{\text{QK}-1} - \text{PQK}+1$
2		718.0			
3	735.3	714.7	1450.0	20.6	
4	739.0	711.5	1450.5	27.5	27.3
5	742.4	708.0	1450.4	34.4	34.6
6	746.0	704.4	1450.4	41.6	41.2
7	749.8	701.2	1451.0	48.6	
8	753.7				
9	757.5				

prolate symmetric top, the following formulae were used for the analysis of both the B and C type bands(47):

$$r_{Q_K} + p_{Q_K} = 2[\nu_0 + (A' - \bar{B}')] + 2 [(A' - \bar{B}') - (A'' - \bar{B}'')]K^2 \text{---(XIII)}$$

$$r_{Q_K} - p_{Q_K} = 4(A' - \bar{B}')K \text{----- (XIV)}$$

$$r_{Q(K-1)} - p_{Q(K+1)} = 4(A'' - \bar{B}'')K \text{----- (XV)}$$

where  $Q_K$  represents the wavenumber of the line of quantum number  $K$  with  $r$  and  $p$  designating the branch.  $\nu_0$  is the band origin.  $A$  is the rotational constant for the A-axis and  $\bar{B} = \frac{1}{2}(B + C)$  where  $B$  and  $C$  are the rotational constants for the B- and C-axes respectively. A double dash indicates that the rotational constant is for the molecule in its ground state and a single dash indicates that the rotational constant is for the molecule in its excited state. A least squares programme run on a Wang Calculator 720B produced the results listed in table 5.

Table 5. Results of Rotational Analysis ( $\text{cm}^{-1}$ )

	$\nu_3$	$\nu_{11}$
$\nu_0$	$2603.77 \pm 0.08$	$723.22 \pm 0.12$
$(A'' - \bar{B}'')$	$1.744 \pm 0.009$	$1.738 \pm 0.050$
$(A' - \bar{B}')$	$1.734 \pm 0.008$	$1.753 \pm 0.008$
$(A' - \bar{B}'') - (A'' - \bar{B}'')$	$-0.0151 \pm 0.0010$	$0.0095 \pm 0.0035$

The large standard deviations in the  $\nu_{11}$  values is caused by few measurable lines being observed in the spectrum. The effective ground state rotational constants for the two vibrations are well within the standard deviations. Solimene and Dailey(27) calculate the rotational constants of  $\text{CD}_3\text{SH}$  from the geometry of the molecule which they determine from microwave data. Their values give  $(A'' - \bar{B}'') = 1.694 \text{ cm}^{-1}$  which probably agrees with the present value obtained from the  $\nu_3$  vibration within the limits of error involved in all work. In particular their value for the C-S-H angle must be suspect since it differs from the value of Kojima(25) by  $4^\circ$ .

## PHOTOLYSIS RESULTS

### Results obtained by E.S.R. spectroscopy

All the E.S.R. experiments had the samples at 77 K and photolysed in situ with a high pressure mercury lamp. The spectra obtained are summarized in tables 6 and 7. The experimental errors are estimated to be  $\pm 2\%$  for the hyperfine splittings and  $\pm 0.4\%$  for the g values.

#### 1. Methanethiol

When pure methanethiol is photolysed a broad anisotropic signal is observed and the sample shows a pale yellow colour in the region of photolysis. The anisotropic signal is seen to change as the sample is rotated. Figures 6a and 6b were obtained by photolysing a  $\text{CH}_3\text{SD}$  sample for thirty minutes in one position, then removing the light source and recording spectra after successive rotations of  $22.5^\circ \pm 2^\circ$ . Thus the seventeenth spectrum was recorded in the same position as the first within a  $\pm 2^\circ$  experimental error. The same behaviour was observed in all five experiments performed using  $\text{CH}_3\text{SH}$ ,  $\text{CH}_3\text{SD}$  or  $\text{CD}_3\text{SH}$  samples. In all cases the spectra recorded in the first and seventeenth positions were very similar, any differences being sufficiently small to be ascribed to the error involved in setting the position of the sample.

Table 6. E.S.R. spectra from pure sulphur compounds irradiated in situ at 77K with high pressure mercury lamp.

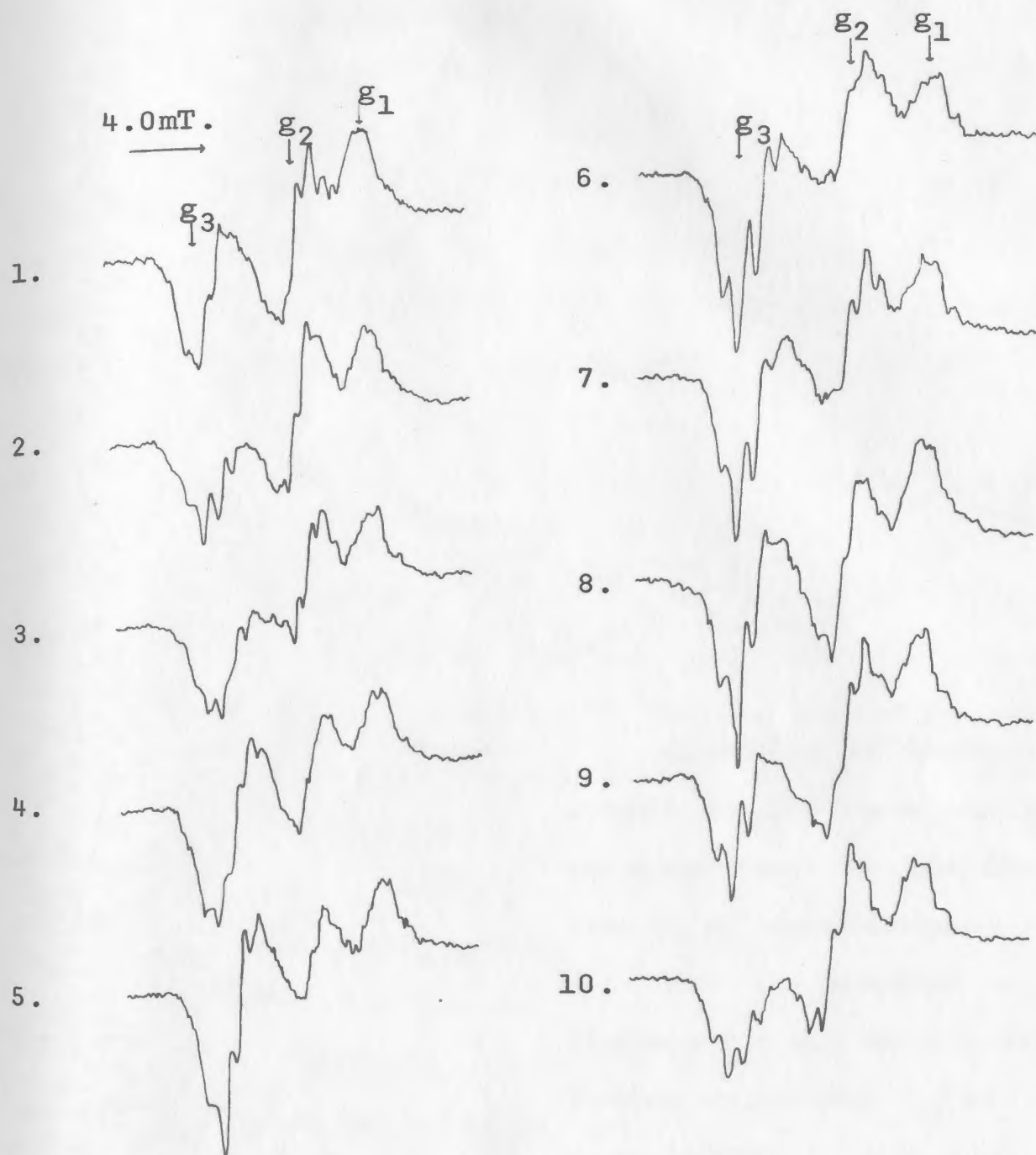
Substrate	Description of signal	Experimental g values and splitting	Frequency (GHz)	Assignment
CH <sub>3</sub> SH	Anisotropic signal with hyperfine splitting. Changes when sample rotated.	$g_1 = 2.002$ ; $g_2 = 2.026$ ; $g_3 = 2.050$ .	9.142	CH <sub>3</sub> S <sup>•</sup>
CH <sub>3</sub> SD	Anisotropic signal with hyperfine splitting. Changes when sample rotated.	$g_1 = 1.998$ ; $g_2 = 2.023$ ; $g_3 = 2.051$ .	9.139	CH <sub>3</sub> S <sup>•</sup>
CD <sub>3</sub> SH	Anisotropic signal with hyperfine splitting. Changes when sample rotated.	$g_1 = 1.998$ ; $g_2 = 2.021$ ; $g_3 = 2.050$ .	9.142	CD <sub>3</sub> S <sup>•</sup>
(CH <sub>3</sub> ) <sub>2</sub> S	Anisotropic signal with hyperfine splitting. No change when sample rotated.	$g_1 = 2.002$ ; $g_2 = 2.027$ ; $g_3 = 2.057$ .	9.141	CH <sub>3</sub> S <sup>•</sup>
	Underlying isotropic quartet.	$g = 2.006$ . Splitting = 2.3 mT.	9.141	CH <sub>3</sub> <sup>•</sup>
	Widely split doublet.	Not measured accurately. $g \approx 2$ ; Splitting $\approx 50$ mT.	9.141	H <sup>•</sup>
(CH <sub>3</sub> ) <sub>2</sub> S <sub>2</sub>	Anisotropic signal with hyperfine splitting. No change upon rotation of sample.	$g_1 = 2.000$ ; $g_2 = 2.022$ ; $g_3 = 2.054$ .	9.141	CH <sub>3</sub> S <sup>•</sup>
	Three lines	$g_1 = 1.988$ ; $g_2 = 2.001$ ; $g_3 = 2.016$ .	9.141	CH <sub>3</sub> SSCH <sub>2</sub> <sup>•</sup>
	Very weak doublet.	Not measured accurately. $g \approx 2$ ; splitting $\approx 50$ mT.	9.141	H <sup>•</sup>

Table 7. Additional E.S.R. signals obtained from irradiated moist methanethiols.

Substrate	Description of signal	g and splitting	Frequency	Assignment
CH <sub>3</sub> SH	Quartet with intensity ratio 1:3:3:1. Seen more readily upon annealing sample.	2.005, 2.3 mT.	9.141	CH <sub>3</sub> <sup>•</sup>
	Doublet.	2.009, 50.1 mT.	9.141	H <sup>•</sup>
CH <sub>3</sub> SD	Quartet with intensity ratio 1:3:3:1. Seen more readily upon annealing sample.	2.005, 2.3 mT.	9.139	CH <sub>3</sub> <sup>•</sup>
	Triplet with intensity ratio 1:2:1. Seen upon annealing when more water present.	2.007, 1.9 mT	9.139	<sup>•</sup> CH <sub>2</sub> SD
	Doublet.	2.010, 50.3 mT.	9.139	H <sup>•</sup>
	Underlying triplet.	1.998, 7.6 mT.	9.139	D <sup>•</sup>
CD <sub>3</sub> SH	Weak underlying septet. Seen more readily upon annealing sample.	2.000, 0.35 mT.	9.144	CD <sub>3</sub> <sup>•</sup>
	Doublet.	2.008, 50.3 mT.	9.144	H <sup>•</sup>
	Weakly underlying triplet.*	Not measured.*	9.144	D <sup>•</sup>

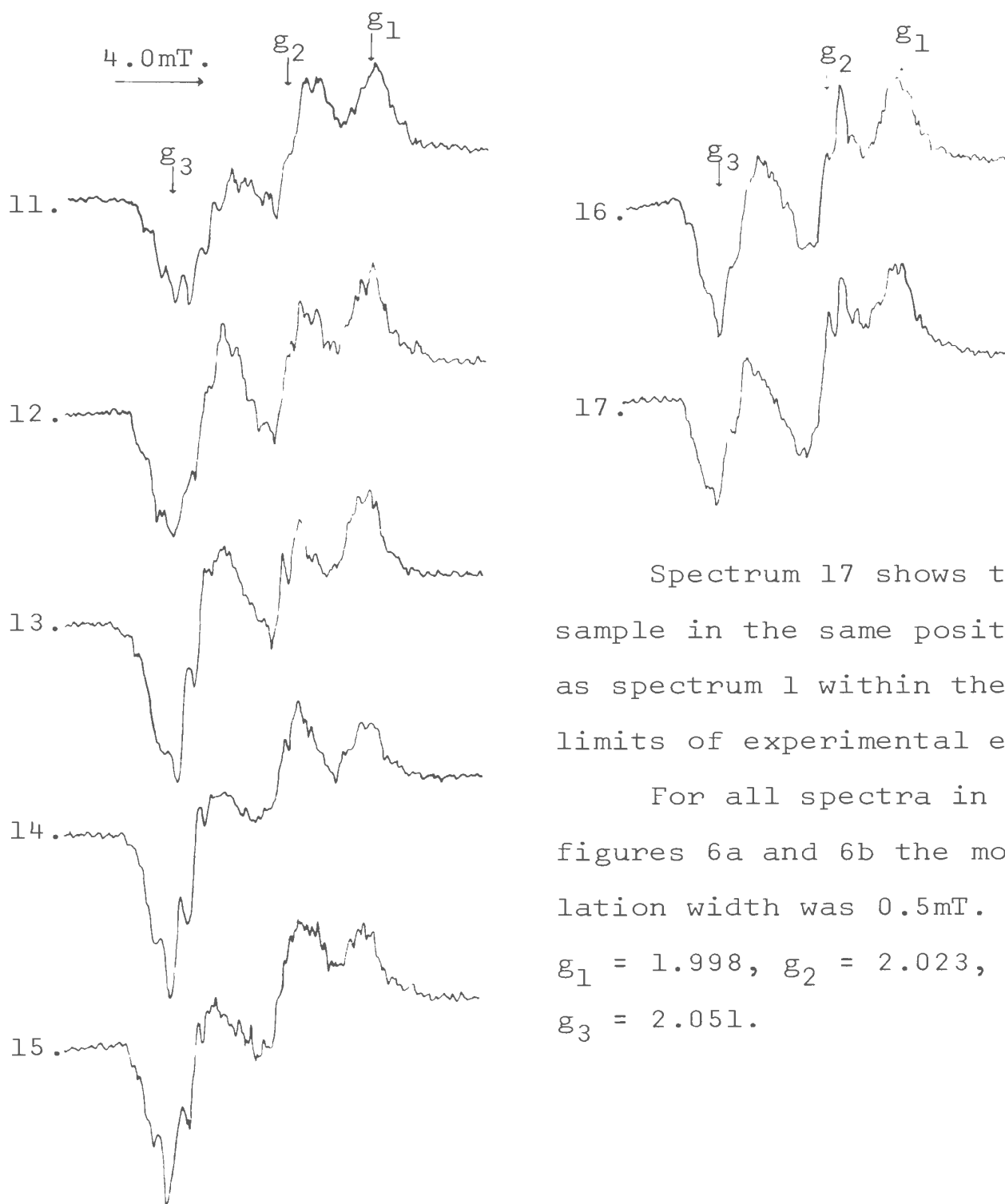
\* High field line only was detected. The other two lines appeared to be masked by the broad anisotropic signal.

Figure 6a: Broad anisotropic E.S.R. signal obtained from photolysed  $\text{CH}_3\text{SD}$ .



Spectra 1-17 in figures 6a and 6b were recorded after successive rotations of the sample by  $22.5^\circ$ .

Figure 6b: Broad anisotropic E.S.R. signal obtained from photolysed  $\text{CH}_3\text{SD}$ .



Spectrum 17 shows the sample in the same position as spectrum 1 within the limits of experimental error.

For all spectra in figures 6a and 6b the modulation width was 0.5mT. and  $g_1 = 1.998$ ,  $g_2 = 2.023$ ,  $g_3 = 2.051$ .

Experiments were performed using glassy samples which gave anisotropic signals, but none of those showed any change upon rotation. (No methyl disulphide or methyl sulphide samples showed any change). This eliminated the possibility that the sample tube or the dewar was causing the change in the signal.

It was found that a small trace of water ( $H_2O$  in the case of  $CH_3SH$  and  $D_2O$  in the case of  $CH_3SD$ ) caused additional E.S.R. signals to appear as listed in table 7. With a sample of  $CH_3SD$  distilled once from a mixture with  $D_2O$ , strong signals were attributed to H atoms, D atoms and  $CH_3\dot{C}$  radicals. In addition a triplet at  $g = 2.007$  with a splitting of 1.9 mT. was observed. With a dryer sample of methanethiol distilled in vacuo from a tube in an ethanol slush bath, the triplet did not appear but the other signals did (although not as strongly). Finally when the sample was allowed to stand over phosphorus pentoxide at 273 K for one hour and then distilled off, only the anisotropic signal was obtained. That the function of the phosphorus pentoxide was to remove water was confirmed by adding a few drops of water to this sample and photolysing again. The additional signals reappeared.

When  $CH_3\dot{C}$  and  $CD_3\dot{C}$  radicals were observed, their spectrum was superimposed on the broad anisotropic

signal and was often difficult to see. A rapid annealing near the melting point of the sample with immediate recooling to 77 K caused a decay of the bulk of the anisotropic signal leaving the methyl signal at approximately its original intensity and hence more easily observed. Figure 7 shows an anisotropic signal from  $\text{CD}_3\text{SH}$  with the region where  $\text{CD}_3^\bullet$  appears being indicated. Figure 8 shows the  $\text{CD}_3^\bullet$  spectrum obtained after the annealing. It is not possible to specifically assign  $\text{CD}_3^\bullet$  peaks in figure 7 since a  $\text{D}^\bullet$  atom peak is expected to be present in this region and also hyperfine splitting of the anisotropic signal is very likely present. The  $\text{CH}_3^\bullet$  and triplet signals obtained from very moist  $\text{CH}_3\text{SD}$  after annealing are shown in figure 9. In some cases a slight increase in the  $\text{CH}_3^\bullet$  signal seemed to occur - perhaps showing the formation of more methyl radicals during the annealing process. The yellow colour formed during photolysis gradually disappeared during the annealing (which was normally done in several steps), and could not be seen after the anisotropic signal had disappeared.

A comparison of the number of the hydrogen atoms produced from sulfhydryl and methyl positions was sought. With this aim a rough estimate of the ratio of the number of unpaired spins associated with  $\text{H}^\bullet$  and  $\text{D}^\bullet$  atoms

Figure 7: E.S.R. signal obtained from moist  $\text{CD}_3\text{SH}$  before annealing.

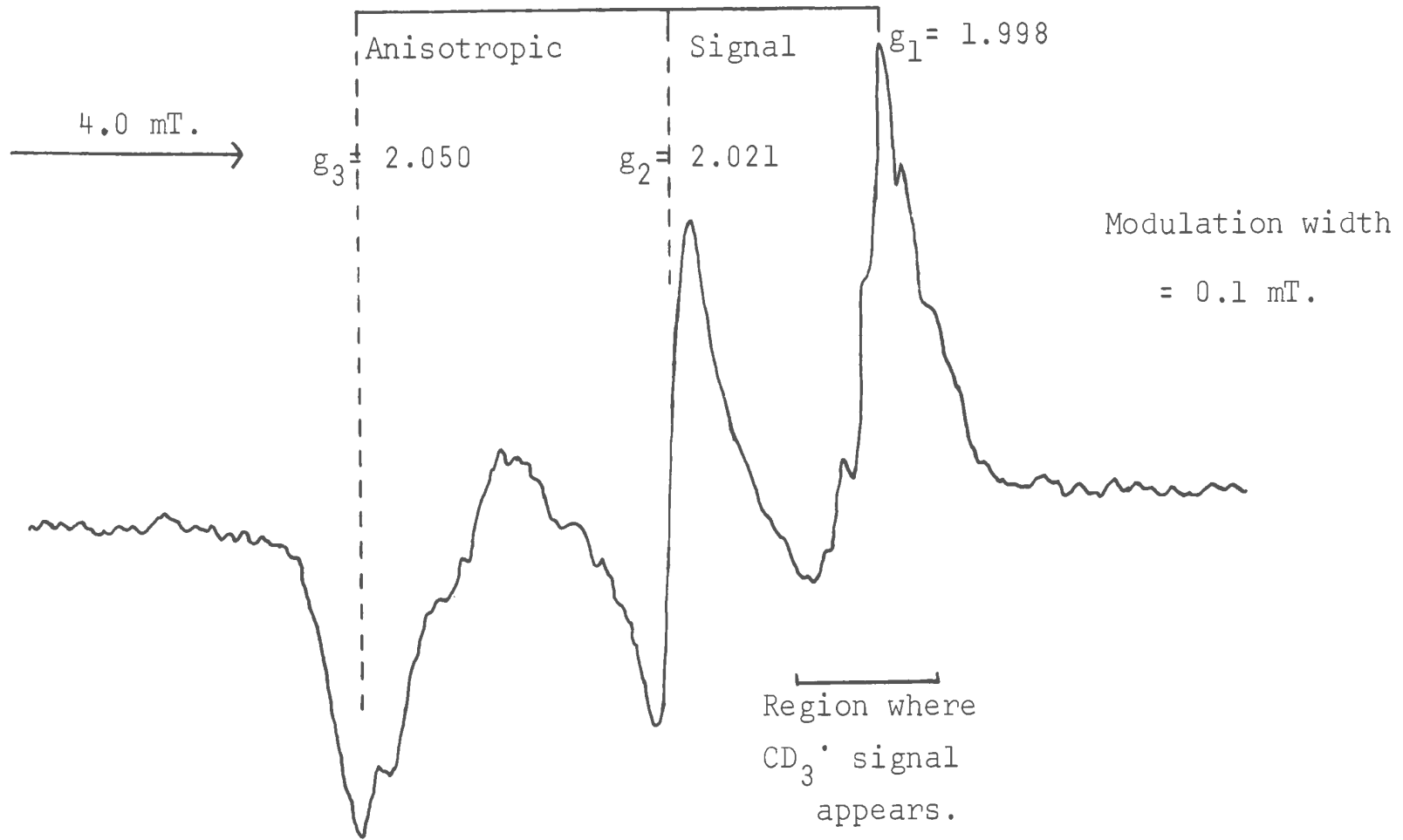


Figure 8:  $\text{CD}_3^\bullet$  signal obtained from moist  $\text{CD}_3\text{SH}$  after annealing.

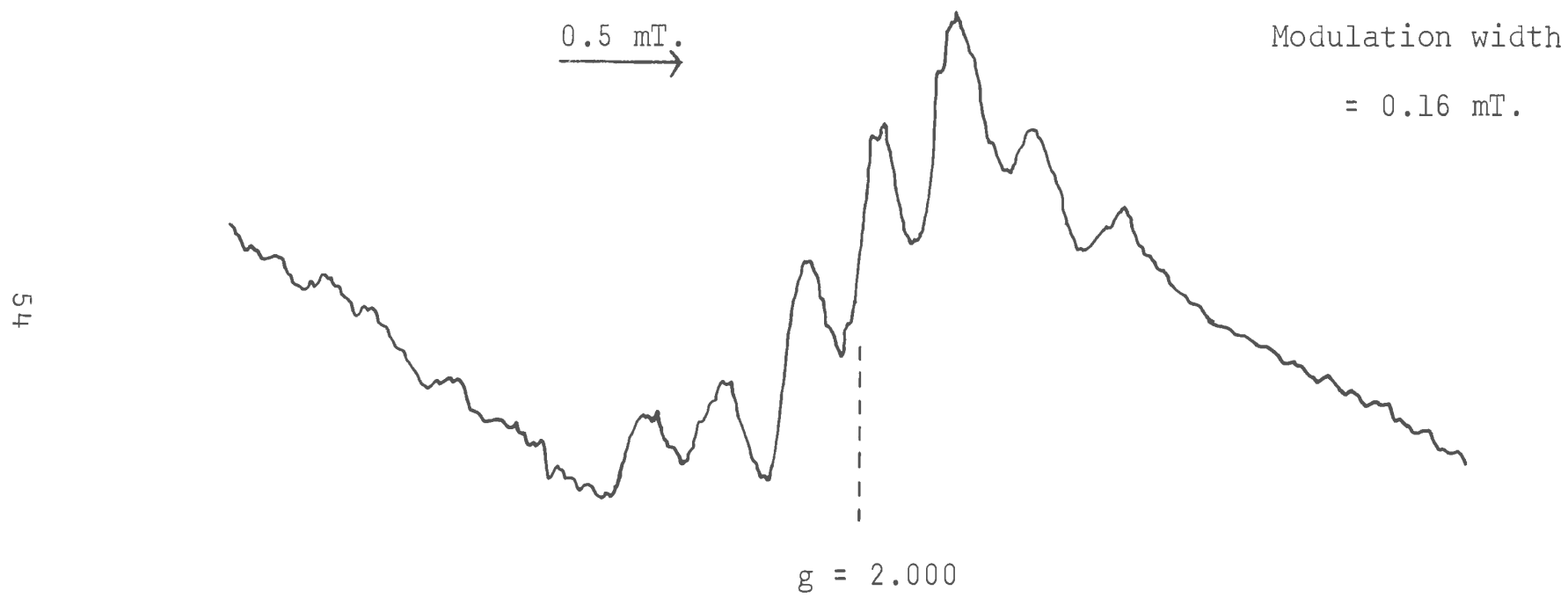
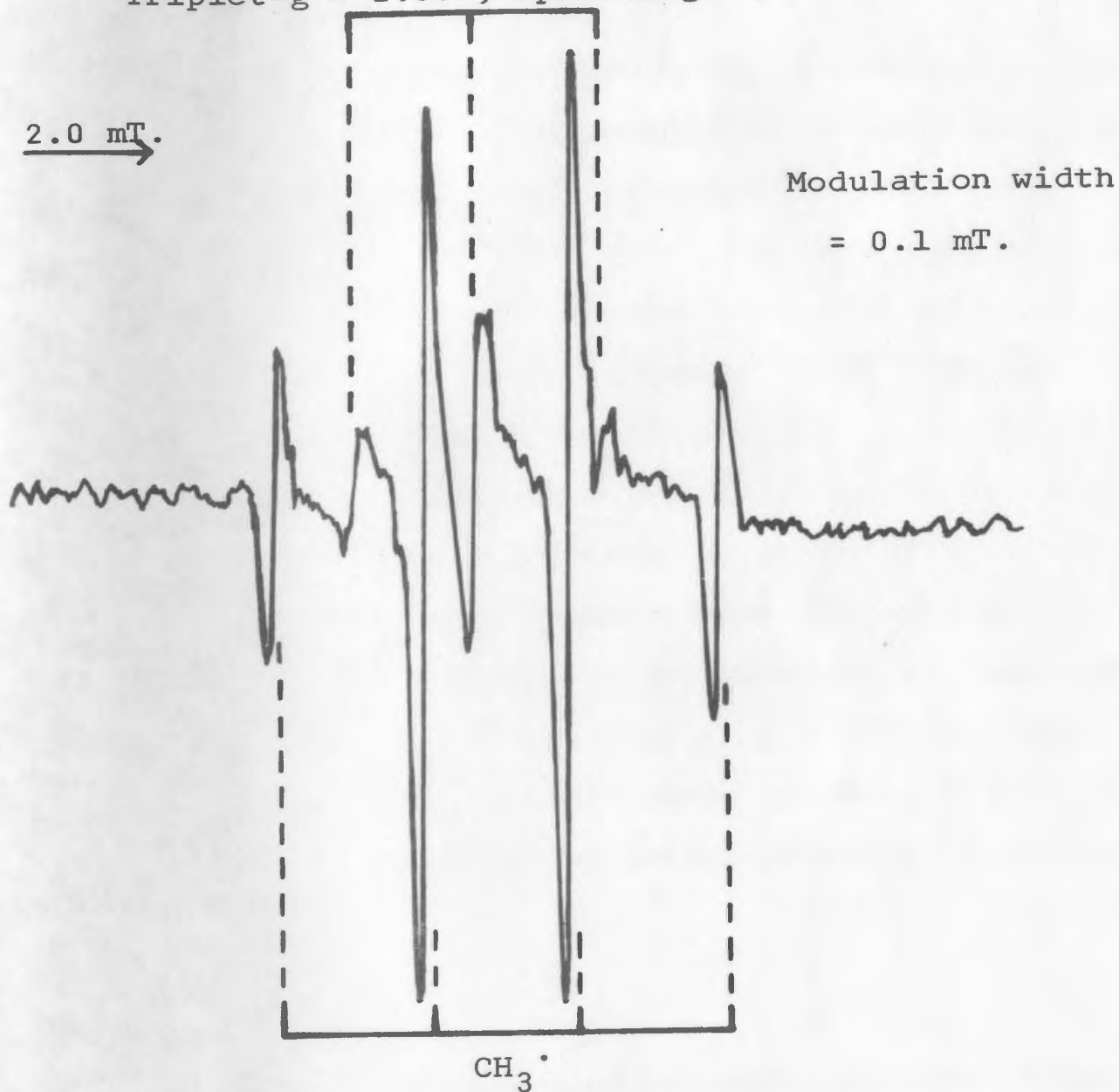


Figure 9: E.S.R. signals obtained from very moist  $\text{CH}_3\text{SD}$  after annealing.

Triplet-g = 2.007; Splitting = 1.9 mT.



$g = 2.005$ ; Splitting = 2.3 mT.

from the partially deuterated methanethiols was made. It was concluded that, of the hydrogen atoms observed, two came from the sulfhydryl position for every one which came from the methyl position.

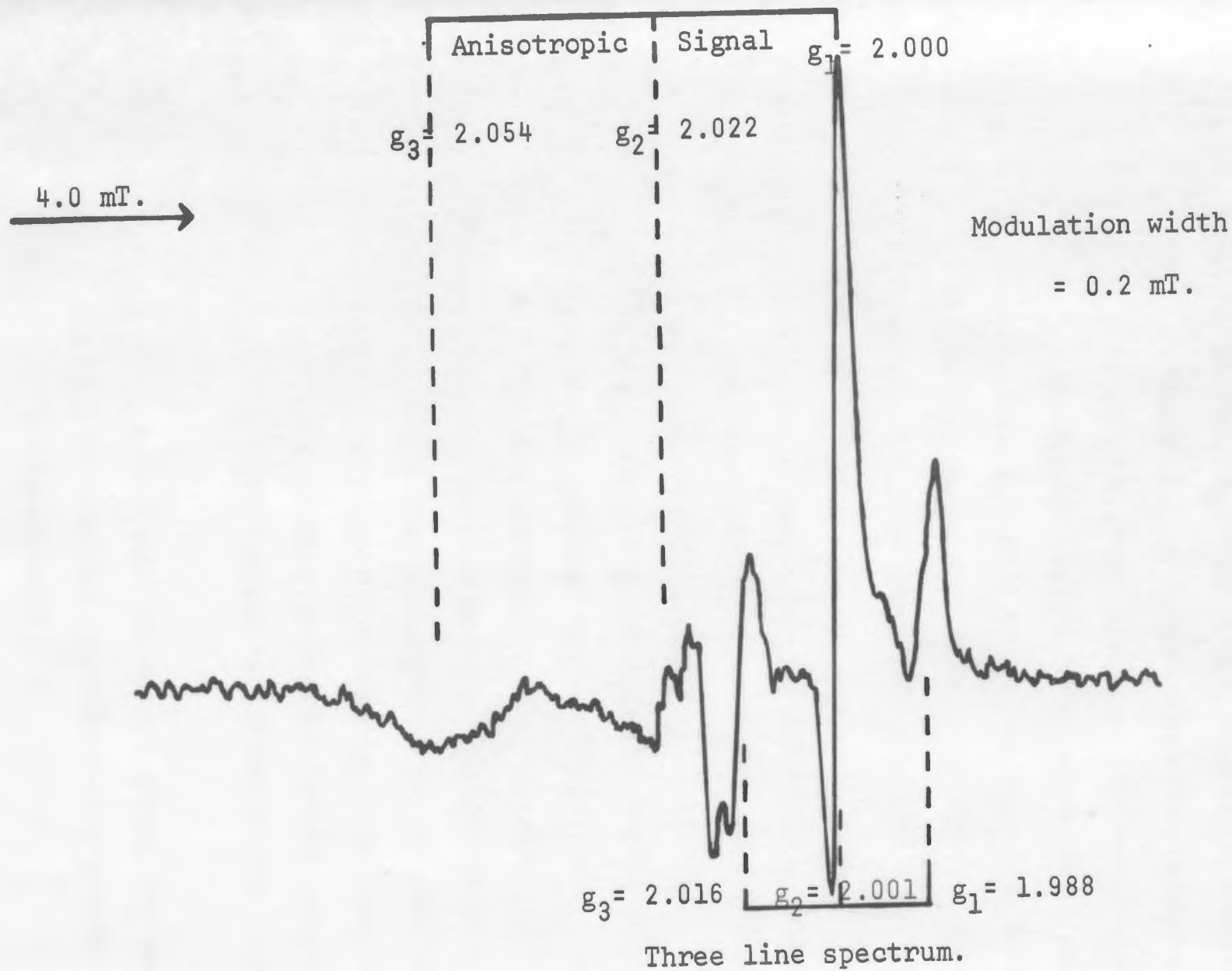
A short series of experiments was performed on the two crystalline phases of methanethiol to check for any difference in the photolysis results. No difference was found.

It was of particular interest to see if an E.S.R. signal could be attributed to sulphur atoms. In the matrix these would be expected to exist in the triplet state with two unpaired electrons in 3p orbitals. For such a species the Landé g-factor is calculated at 1.5. A half-field transition (in which both electron spins are simultaneously reversed) is expected to be less broad and hence more readily detectable at  $g = 3$  (33). Very careful scans at high gain were made in the  $g = 1.5$  and  $g = 3$  regions but no signal could be detected in either case.

## 2. Methyl disulphide

When photolysed, methyl disulphide showed a violet colour in the region of photolysis and the E.S.R. spectra listed in table 6 were obtained. A broad anisotropic

Figure 10: E.S.R. spectrum obtained from photolysed methyl disulphide.

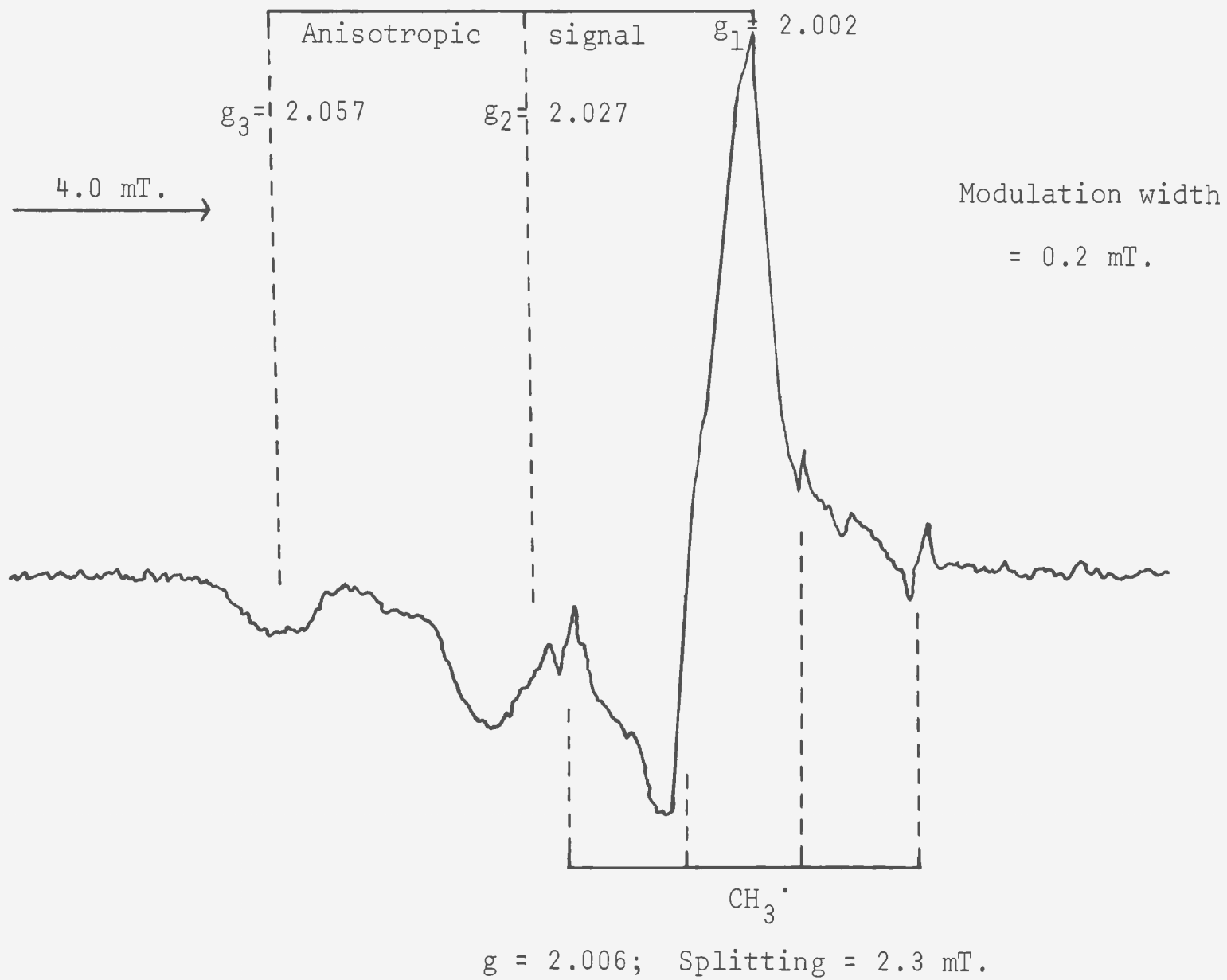


signal similar to that from methanethiol appeared (figure 10) but no change was observed upon rotating the sample. Superimposed on this spectrum were lines which are interpreted as a second anisotropic signal but which were very close to an isotropic triplet with a splitting of 1.95 mT. No evidence for methyl radicals was found, but this quartet would be difficult to see in the presence of the two other signals.

A series of rapid annealings near the melting point of the disulphide showed the three line spectrum to decay much more quickly than the broad anisotropic signal. During the annealing the violet colour disappeared at an early stage leaving a faint yellow colour which was probably present before, but masked by the violet colour. With further annealing the yellow colour disappeared. As close as could be judged the disappearance of the violet colour occurred with the decay of the three-line spectrum, and the yellow colour disappeared with the broad anisotropic signal. No new spectra appeared during the annealing process.

No change in the results was observed when the methyl disulphide was allowed to stand over phosphorus pentoxide for an hour prior to the experiment.

Figure 11: E.S.R. spectrum obtained from photolysed methyl sulphide.



### 3. Methyl sulphide

Photolysis of methyl sulphide produced a faint yellow colour and the E.S.R. spectra listed in table 5. The broad anisotropic signal (figure 11) was similar to those observed from methanethiol and methyl disulphide and it showed no change upon rotation of the sample. With repeated rapid annealings the features attributed to methyl radicals were found to decay before the anisotropic signal. The yellow colour again disappeared as the anisotropic signal decayed.

#### Results obtained from infrared spectroscopy

All the argon matrix experiments were carried out in their entirety at 17 K. For the experiments without argon the deposition was carried out at 77 K and the window then cooled to 17 K before recording spectra and photolysing. Results show intensity of absorptions at different frequencies before and after photolysis for  $\text{CH}_3\text{SH}$  (table 8),  $\text{CD}_3\text{SH}$  (table 9),  $\text{CH}_3\text{SSCH}_3$  (table 10) and  $\text{CH}_3\text{SCH}_3$  (table 11).

The lines in the argon matrix experiments were generally very narrow and well defined and should in no case have an experimental error greater than  $\pm 2 \text{ cm}^{-1}$ . In contrast the absorptions of the pure methanethiols

Table 8. Absorption bands recorded before and after photolysis of CH<sub>3</sub>SH.

Experiment with CH <sub>3</sub> SH in Argon matrix (ratio 250:1).				Experiment using pure CH <sub>3</sub> SH with no inert gas matrix.			
$\nu$ (cm <sup>-1</sup> )	Before photolysis	After 2 hours photolysis with H.P. Hg. lamp	Assignment	Before photolysis	After 2 hours photolysis with L.P. Hg. lamp	After further 30 minutes photolysis with H.P. Hg. lamp	$\nu$ (cm <sup>-1</sup> )
3024		sh	D				
3010		sh	CH <sub>4</sub>				
3005	0.39	0.31	CH <sub>3</sub> SH	0.4	0.4	0.4	2996
2967	0.04	0.13	CH <sub>3</sub> SH plus?				
2960		0.05	B				
2947	0.77	0.53	CH <sub>3</sub> SH	0.9	0.8	0.6	2925
2935	sh	sh	CH <sub>3</sub> SH				
2877	0.08	0.05	CH <sub>3</sub> SH	0.10	0.08	0.06	2860
2868		sh	D				
2854	0.13	0.07	CH <sub>3</sub> SH	0.15	0.13	0.12	2833
2550 br.	0.07	0.05	CH <sub>3</sub> SH	0.95	0.8	0.7	2534
2176		0.04	CS <sub>2</sub>				
2136 db		0.02	CO				
2051	0.05	0.03	CH <sub>3</sub> SH				
1745		0.05	D				
1528		1.7	CS <sub>2</sub>		0.05	0.22	1513
1477		0.05	B				
1473		0.025	B				
1445	0.69	0.37	CH <sub>3</sub> SH				
1436	0.62	0.42	CH <sub>3</sub> SH	0.75	0.69	0.66	1430 v.br.
1422	sh	sh	CH <sub>3</sub> SH				
1326	0.39	0.31	CH <sub>3</sub> SH	sh	sh	sh	1410
1304		0.40	CH <sub>4</sub>	0.29	0.28	0.27	1318
1275		0.25	CS		0.15	0.27	1299
1269		0.04	CS				
1180		0.01	A				
1172	0.03	0.03	Impurity		0.01	0.01	1160
1096	0.02	0.01	Impurity				
1068	0.77	0.42	CH <sub>3</sub> SH				
1062		0.11	B	0.80	0.72	0.69	1065
1055		0.05	A		0.01	0.01	1033
1031	0.03	0.03	Impurity				
993 db		0.32	D				
987		0.24	A + D?				
954	0.41	0.26	CH <sub>3</sub> SH	0.64	0.60	0.57	961
799	0.20	0.14	CH <sub>3</sub> SH	0.17	0.17	0.17	801
735		0.015	A				
703	0.29	0.21	CH <sub>3</sub> SH	0.53	0.46	0.41	701
533 br		0.02	B				
391 br		0.02	CS <sub>2</sub>				

In tables 8 - 11 the following abbreviations are used.

sh = shoulder; br = broad; v. br. = very broad; db = doublet

Table 9. Absorption bands recorded before and after photolysis of CD<sub>3</sub>SH.

Two experiments using argon matrix.					Experiment without inert matrix.				
ν (cm <sup>-1</sup> )	1:250 Ratio		1:500 Ratio		Assignment	1½ hr.	+½ hr.	ν (cm <sup>-1</sup> )	
	H.P. Lamp		L.P. Lamp			photo	photo		
	No	2 hr.	No	2 hr.		No	L.P.		H.P.
	photo	photo	photo	photo		Lamp	Lamp		
2599	0.02	0.01	0.01		CD <sub>3</sub> SH	0.04	0.03	0.03	2640
						sh	sh	sh	2550
						1.6	1.3	1.1	2530
2259	0.09	0.03	0.04	0.03					
2254	0.09	0.03	0.04	0.03	CD <sub>3</sub> SH	0.12	0.11	0.10	2250
2234		0.66					sh	sh	2240
2174		0.04			CS <sub>2</sub>				
2155		0.07							
2146	0.22	0.10	0.15	0.13	CD <sub>3</sub> SH	0.25	0.21	0.19	2135
2138		0.05							
2100	0.03	0.02	0.03	0.02	CD <sub>3</sub> SH				
2080	0.03	0.02	0.03	0.02	CD <sub>3</sub> SH				
2049		0.05		0.01					
							0.01	0.03	1840 br
1747		0.02							
1733				0.02					
1532		sh							
1528		1.6		0.15	CS <sub>2</sub>	0.02	0.17		1513
1523		sh		sh					
1521				0.02					
1477		0.02							
					CD <sub>3</sub> SH	0.02	0.02	0.02	1435 br
1290		0.21			CD <sub>3</sub> H				
1280		0.03							
1275		0.57		0.06				0.04	1277
1269		0.17		0.04	CS				
1264		0.03							
1259		0.03							
1172		sh							
1171		0.05							
1167		0.03							
1055	0.23	0.14	0.21	0.19	CD <sub>3</sub> SH	0.54	0.48	0.45	1045
1046	0.24	0.12	0.21	0.15					
1038br		0.04							
1029br		0.02					sh	sh	1028
1015	0.22	0.08	0.13	0.11	CD <sub>3</sub> SH	0.16	0.11	0.10	1012
1000		0.02					0.01	0.01	1000
991		0.06							
977	0.17	0.04	0.07	0.05	CD <sub>3</sub> SH	0.13	0.11	0.10	982
						0.13	0.11	0.10	962
							sh	sh	970
937		0.02					0.01	0.02	940
894		0.135		0.02					
							0.01	0.02	822
783		0.31		0.02					
779		0.15		0.01					
738br		0.02					0.01	0.02	758
724	0.13	0.03	0.06	0.04	CD <sub>3</sub> SH	0.28	0.24	0.21	733
					CD <sub>3</sub> SH	0.24	0.17	0.14	688
643	0.23	0.06			CD <sub>3</sub> SH	0.81	0.52	0.41	643
615vbr		0.02							
588		0.10					0.01	0.01	570
573		0.02							
397br		0.02							

Table 10. Absorption bands recorded before and after photolysis of methyl disulfide in argon. Matrix ratio was 1:250 and a high pressure mercury lamp was used.

$\nu$ ( $\text{cm}^{-1}$ )	Before photolysis	After 1.5 hours photolysis	Assignment
3015		sh?	$\text{CH}_4?$
3006		sh	$\text{CH}_3\text{SH}$
3000	0.17	0.08	$(\text{CH}_3)_2\text{S}_2$
2967		0.015	$\text{CH}_3\text{SH}$ plus?
2960		0.03	B
2947		0.03	$\text{CH}_3\text{SH}$
2931	0.75	0.48	$(\text{CH}_3)_2\text{S}_2$
2874		0.01	$\text{CH}_3\text{SH}$
2855	0.06	0.04	$(\text{CH}_3)_2\text{S}_2$
2824	0.08	0.05	$(\text{CH}_3)_2\text{S}_2$
2173		0.03	$\text{CS}_2$
1749 db		0.05	E
1532		sh	E
1527		2.0	$\text{CS}_2$
1523		sh	E
1505		0.02	E
1477		0.03	B
1473		0.01	B
1446		0.02	$\text{CH}_3\text{SH}$
1441		0.09	E
1436	2.0	0.58	$(\text{CH}_3)_2\text{S}_2$
1430		sh?	E
1423		sh	E
1421	0.45	0.26	$(\text{CH}_3)_2\text{S}_2$
1419		sh	E
1414	0.70	0.30	$(\text{CH}_3)_2\text{S}_2$
1326		0.015	$\text{CH}_3\text{SH}$
1305	0.77	0.38	$(\text{CH}_3)_2\text{S}_2$
1302		sh?	$\text{CH}_4?$
1275		0.02	CS
1269		0.01	CS
1217		0.10	E
1178		0.01	A
1100		0.01	E
1066		0.05	$\text{CH}_3\text{SH}$
1062		sh	B
1055		0.05	A
1052		0.06	E
1000		0.10	E
995		sh	E
987		0.07	A
956	1.1	0.57	$(\text{CH}_3)_2\text{S}_2$
948	sh	sh	E
946	0.21	0.12	$(\text{CH}_3)_2\text{S}_2$
764	0.02	sh	$(\text{CH}_3)_2\text{S}_2$
761		0.10	E
751		0.03	E
747		sh?	E
735		0.025	A
704		0.11	E
702		sh	$\text{CH}_3\text{SH}$
692	0.21	0.11	$(\text{CH}_3)_2\text{S}_2$
613		0.01	613
552		0.04	B
397 br		0.02	$\text{CS}_2$

Table 11. Absorption bands recorded before and after photolysis of methyl sulphide in argon. Matrix ratio was 1:250 and a high pressure mercury lamp was used.

$\nu$ ( $\text{cm}^{-1}$ )	Before photolysis	After 2 hours photolysis	After 4 hours photolysis	Assignment
3011		0.096	0.110	$\text{CH}_4$
2997	0.36	0.29	0.25	$(\text{CH}_3)_2\text{S}$
2972	0.63	0.45	0.40	$(\text{CH}_3)_2\text{S}$
2925 db	1.18	0.82	0.74	$(\text{CH}_3)_2\text{S}$
2885	0.094	0.07	0.07	$(\text{CH}_3)_2\text{S}$
2866	0.28	0.17	0.15	$(\text{CH}_3)_2\text{S}$
2856	0.16	0.08	0.07	$(\text{CH}_3)_2\text{S}$
2838	0.35	0.19	0.18	$(\text{CH}_3)_2\text{S}$
2135		0.020	0.033	CO
2090 db		0.027	0.030	F
1528		0.65	0.79	$\text{CS}_2$
1446	0.34	0.28	0.26	$(\text{CH}_3)_2\text{S}$
1440	1.4	0.90	0.79	$(\text{CH}_3)_2\text{S}$
1432	1.6	0.95	0.84	$(\text{CH}_3)_2\text{S}$
1361		0.01	0.02	F
1311	0.35	0.26	0.23	$(\text{CH}_3)_2\text{S}$
1304		0.41	0.46	$\text{CH}_4$
1275		0.015	0.015	CS
1269		0.01	0.01	CS
1180		0.01	0.01	A
1055		0.021	0.023	A
1033	sh	sh	sh	$(\text{CH}_3)_2\text{S}$
1030	1.2	0.78	0.68	$(\text{CH}_3)_2\text{S}$
987		0.045	0.042	A
977	0.16	0.11	0.10	$(\text{CH}_3)_2\text{S}$
973	0.7	0.46	0.43	$(\text{CH}_3)_2\text{S}$
900	0.1	0.06	0.05	$(\text{CH}_3)_2\text{S}$
735		0.025	0.023	A
695	0.35	0.25	0.26	$(\text{CH}_3)_2\text{S}$

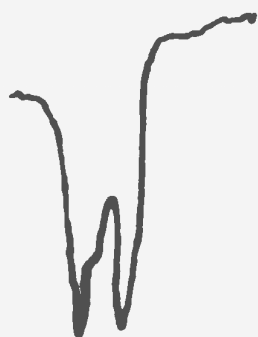
were broad (typical of the spectra of unannealed solids) and accordingly the uncertainty is larger; it is estimated at a maximum of  $\pm 4 \text{ cm}^{-1}$ . Figures 3 and 4 show the two typical types of spectra. It should be emphasized that the quoted uncertainties are an estimated maximum and that many frequencies will be somewhat more precisely fixed. For instance most of the new absorptions had their frequencies checked directly against the spectrometer wavenumber scale and hence no error is involved in extrapolating frequencies on the recorded spectra for these lines.

The absorptions at  $993 \text{ cm}^{-1}$  and  $987 \text{ cm}^{-1}$  in the  $\text{CH}_3\text{SH}$  spectra are similar to those at  $783 \text{ cm}^{-1}$  and  $779 \text{ cm}^{-1}$  in the  $\text{CD}_3\text{SH}$  spectra. They may well be features of one vibrational mode showing an isotopic shift. The weaker  $987 \text{ cm}^{-1}$  absorption which appears upon photolysis of methyl disulphide and methyl sulphide is quite possibly present in the  $\text{CH}_3\text{SH}$  spectra (i.e. two absorptions may be produced at  $987 \text{ cm}^{-1}$  in the  $\text{CH}_3\text{SH}$  spectra).

The spectra of pure solid  $\text{CD}_3\text{SH}$  show considerable crystal-field splitting of the  $\nu_6$  vibration before photolysis (figures 3 and 12). Upon photolysis a new absorption grows between the two main peaks of the  $\nu_6$  mode, and upon warming the sample the new absorption

Figure 12: The  $\nu_6$  band of solid  $\text{CD}_3\text{SH}$ .

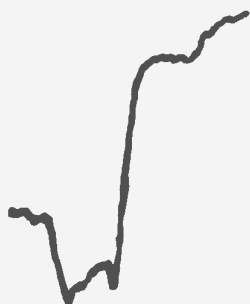
(i) Before photolysis



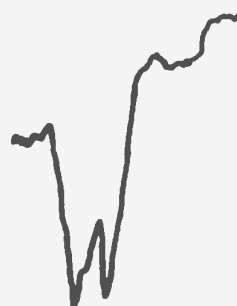
(ii) After  $1\frac{1}{2}$  hours photolysis with L.P. Hg lamp.



(iii) After a further  $\frac{1}{2}$  hour photolysis with H.P. Hg lamp.



(iv) As sample was warmed after photolysis.



In all the diagrams transmittance is the vertical axis and wavenumber is the horizontal axis. The left absorption peak is at  $982\text{ cm}^{-1}$  and the right absorption peak at  $962\text{ cm}^{-1}$ .

decays before the  $\nu_6$  mode. Accordingly table 8 shows 970  $\text{cm}^{-1}$  (approximately) as a new species with 982 and 962  $\text{cm}^{-1}$  attributed to the  $\nu_6$  mode of  $\text{CD}_3\text{SH}$ .

## DISCUSSION

### Assignment of E.S.R. spectra

Assignment of E.S.R. signals to hydrogen atoms, deuterium atoms, and methyl radicals has already been made easily and without ambiguity. Methyl-d<sub>3</sub> radicals are expected to show a seven line spectrum with intensity ratios 1:3:6:7:6:3:1. The spectrum in figure 8 attributed to CD<sub>3</sub><sup>•</sup> shows seven lines whose intensity ratio is close to this but cannot be measured exactly due to underlying signals. There is little doubt that this assignment is correct.

### The anisotropic signal

The broad anisotropic signal which appears in all present experiments always has the same g-factors within the limits of experimental error and is similar to signals observed by other workers (12, 13, 34, 35, 36) and attributed to thiyl radicals. The present signal is accordingly attributed to CD<sub>3</sub>S<sup>•</sup> (CD<sub>3</sub>SH experiments) and CH<sub>3</sub>S<sup>•</sup> (all other experiments). Reports of signals attributed to HS<sup>•</sup> and DS<sup>•</sup> radicals have been made (37). Since both of these appear in the same region as the thiyl radicals, the possibility of their presence in the methanethiol experiments cannot be excluded.

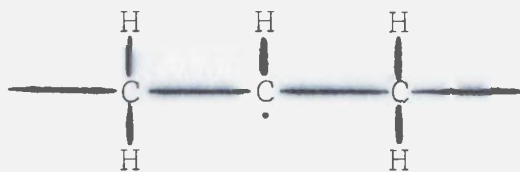
## The three line spectrum from methyl disulphide

The three lines obtained in the methyl disulphide experiments are interpreted as an anisotropic signal but are very close to an isotropic triplet. By cleavage of a C-S or C-H bond (by direct photolysis or an abstraction reaction) the disulphide would give rise to  $\text{CH}_3\text{SS}^\bullet$  or  $\text{CH}_3\text{SSCH}_2^\bullet$  radicals respectively. The possibility of either of these species being carriers of the three-line spectrum will therefore be considered.

Radicals which have the spin of the unpaired electron concentrated on a sulphur atom are expected to show spin-orbit coupling resulting in a g-factor approximately 1% higher than the free spin value (38). The observed signal was centered at  $g = 2.001 \pm 0.008$  which is not consistent with the predicted g-factor of 2.02 for a sulphur radical such as  $\text{CH}_3\text{SS}^\bullet$ .

An alkyl radical such as  $\text{CH}_3\text{SSCH}_2^\bullet$  however would be expected to give rise to a signal near the free spin g-factor. Hyperfine interaction would be expected to occur with the two  $\alpha$ -protons and this would be expected to show both isotropic and anisotropic components of comparable magnitude (39). With a randomly oriented sample the anisotropic interaction results in line broadening and the observed spectrum appears to arise

mainly from the isotropic interactions (40). The assignment of the three-line spectrum to  $\text{CH}_3\text{SSCH}_2\cdot$  therefore seems reasonable. It may be noted that Windle, Wiersema and Tappel (13) have interpreted 8-line spectra centered at  $g= 2.003$  as alkyl radical signals where the alkyl radicals were of the type



and contained sulphur atoms. Their work would seem to support the present assignment.

The triplet obtained from very moist  $\text{CH}_3\text{SD}$ .

Volman et al. investigated the photolysis of methanethiol in aqueous solution at 77K using a high pressure mercury lamp (12). They obtained a triplet similar to that obtained from very moist  $\text{CH}_3\text{SD}$  in the present work. They did not report a g-factor, but judging by its position relative to the methyl signal the triplet which they observed is in approximately the same position as the present one and the splittings are similar. Their assignment of  $\cdot\text{CH}_2\text{SH}$  seems reasonable and supports the assignment of the present triplet to  $\cdot\text{CH}_2\text{SD}$  (which is expected to have the same E.S.R.

spectrum as  $\cdot\text{CH}_2\text{SH}$ ). produced upon photolysis of the undeuterated species have therefore been designated by Assignment of infrared spectra a capital letter according to which species they arise from.

The absorptions listed in tables 8-11 are numerous and, in many cases, rather weak. It has been possible to make assignments in some cases on the basis of established frequencies and the effect of deuteration. These are listed in the appropriate columns of the tables. It might be noted that the CS species has been reported at  $1274\text{ cm}^{-1}$  (41). It seems likely that two lines which appear at  $1269\text{ cm}^{-1}$  and  $1275\text{ cm}^{-1}$  in all the present argon matrix experiments should be attri-

buted to the vibration of this species. In the experiments without an isolation matrix a single broader absorption at  $1277\text{ cm}^{-1}$  is identified with CS.

Despite literature searches for the fundamentals of various species whose presence might be expected, no further assignments have been possible. In some cases the reported fundamentals were not found in the present work (e.g. hydrogen sulphide) while in many other cases no record of the fundamentals was available (e.g. thioformaldehyde). Assignments from chemical evidence or anticipated spectral frequencies is not possible due to the large number of carriers present.

1) Most of the infrared results were obtained from

The unassigned lines produced upon photolysis of the undeuterated species have therefore been designated by a capital letter according to which species they arise from. Table 12 shows the designations used in tables 8, 10, and 11. These unassigned lines will be discussed further at a later stage.

Table 12: Designations used for the unassigned absorptions appearing in tables 8, 10, and 11.

When absorption arises from	Designation used
$\text{CH}_3\text{SH}$ , $\text{CH}_3\text{SSCH}_3$ and $\text{CH}_3\text{SCH}_3$	A
$\text{CH}_3\text{SH}$ and $\text{CH}_3\text{SSCH}_3$ only	B
$\text{CH}_3\text{SH}$ and $\text{CH}_3\text{SCH}_3$ only	C
$\text{CH}_3\text{SH}$ only	D
$\text{CH}_3\text{SSCH}_3$ only	E
$\text{CH}_3\text{SCH}_3$ only	F

### Decomposition mechanisms

At this point it must be emphasised that

i) Most of the infrared results were obtained from

argon matrix experiments whereas the E.S.R. experiments had no inert matrix present.

ii) In some of the infrared experiments a low pressure mercury lamp was used whereas a high pressure mercury lamp (providing more energetic radiation) was used in all the E.S.R. experiments. Moreover when a high pressure mercury lamp was used in the infrared experiments it was a different lamp and possibly had a different distribution of wavelengths.

iii) The optical arrangements for photolysis differed in the two series of experiments.

iv) All the E.S.R. experiments were run at 77K, all the infrared experiments were at 17K.

Due to the differences between the two series of experiments, it is possible that when two or more decomposition paths can occur the one which predominates in the E.S.R. experiments may be of minor importance in the infrared. Care must therefore be taken in any attempt to combine results from the two series of experiments.

The full decomposition mechanisms are obviously very complex with secondary photolysis and various chemical reactions occurring. This section will suggest some processes which occur within the full mechanisms.

## Decomposition mechanism of methanethiol

### The primary photolytic step

Methanethiol has been subjected to various types of radiation in the gaseous and solid phases (1, 6-12). It is generally accepted that S-H cleavage is the most important primary photolytic step

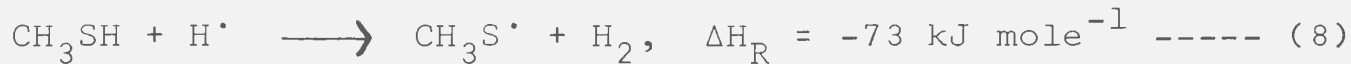


although some workers (11, 12) do not exclude the possibility of some primary photolysis being via cleavage of the C-S bond



In any event since only three different kinds of bond are present in the substrate, the primary photolysis must yield H<sup>·</sup> atoms (S-H cleavage), CH<sub>3</sub><sup>·</sup> radicals (C-S cleavage), H<sup>·</sup> atoms and <sup>·</sup>CH<sub>2</sub>SH radicals (C-H cleavage) or some combination of these. In the present E.S.R. experiments on pure dry methanethiol none of these are detected so that whichever is produced must undergo some rapid reaction. Since experiments with a trace of water present show both H<sup>·</sup> and CH<sub>3</sub><sup>·</sup> it is likely that they are both produced in perfectly dry methanethiol (although not necessarily both by a primary

photolysis) but undergo a rapid abstraction reaction with substrate molecules (42)



where  $\Delta H_{\text{R}}$  for these and all subsequent equations is the heat of reaction calculated from standard heats of formation (at 298K) available in the literature (43).

#### The effect of water

The observation of  $\text{CH}_3\cdot$  and  $\text{H}\cdot$  in samples with a trace of water would then indicate that the abstraction reactions could not occur so readily in this case. Volman et al (12) observed  $\text{CH}_3\cdot$  and  $\text{H}\cdot$  in photolysed aqueous solutions of methanethiol. They suggest that the water hydrogen bonded with the sulfhydryl groups of the substrate molecules and so prevented the abstraction reactions. Whether there was sufficient water present in the current experiments to impede thus the abstraction reactions sufficiently to make  $\text{CH}_3\cdot$  and  $\text{H}\cdot$  observable is dubious, since the  $\text{CH}_3\cdot$  and  $\text{H}\cdot$  signals could be observed when a sample of methanethiol was taken from a commercial bottle and distilled in vacuo before use. Further, it must be expected that hydrogen

atoms in the lattice will be quite mobile and hence rapidly able to locate a free sulfhydryl group if some existed. However it is difficult to offer an alternative explanation of this phenomenon at the present time.

The detection of  $\cdot\text{CH}_2\text{SD}$  radicals from a very moist sample of  $\text{CH}_3\text{SD}$  would be explained by Volman et al (12) as arising from an alternative abstraction process involving substrate molecules whose sulfhydryl groups were strongly bonded to water:



No thermochemical data is available for these reactions but they are expected to be energetically feasible. Again no alternative explanation can be given.

#### Formation of carbon monosulphide

The observation of deuterium atoms from moist  $\text{CD}_3\text{SH}$  indicates cleavage of a C-D bond. It is likely that this also occurred in the perfectly dry compounds used in E.S.R. experiments. The observation of CS in the methanethiol infrared experiments indicates that all C-H or C-D bonds were broken in that case. It is unlikely

that C-H cleavage occurred as a primary photolysis so the following mechanism is proposed as the route to CS in all experiments.



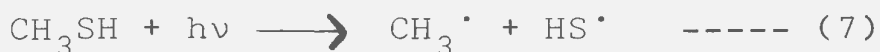
The ultraviolet spectra of  $\text{CH}_3\text{S}^\cdot$  and  $\text{CH}_2\text{S}$  (1) indicate that photolysis of these species may occur. Reaction 13 may take place in two steps via  $\text{CHS}^\cdot$ . For the E.S.R. experiments at least it is preferred as written since (i) no signal attributed to  $\text{CHS}^\cdot$  was observed (a doublet similar to the  $\text{CHO}^\cdot$  doublet with a 13.6 mT. splitting (46) would be expected), (ii) the sulfhydryl to methyl hydrogen atom ratio of 2:1 indicates fewer methyl hydrogens than would probably arise if reaction 13 occurred in two steps. With the lower energy radiation of the low pressure lamp (used in some infrared experiments) however, a two step process becomes more likely. Concerning reactions 2 and 12, it is probable that the disproportionation is more important in the matrix isolation experiments than in the pure solid.

## Formation of carbon disulphide and methane

Carbon disulphide and methane are identified as products in all the infrared experiments. It is extremely likely that they are also formed in the E.S.R. experiments. Methyl radicals were observed in moist methanethiol and are expected to be present as a precursor to methane in all experiments. The carbon disulphide is expected to arise by carbon monosulphide acquiring a sulphur atom which may be a free atom or may be abstracted from some other species. It is noted that the solid phase photolysis of carbonyl sulphide failed to produce an E.S.R. signal attributed to sulphur atoms (44). In that work it was concluded that sulphur atoms were present, but were small enough to be very mobile and hence able to dimerize rapidly (33, 44). Since a similar situation may well apply in the present case, two possible mechanisms for the formation of carbon disulphide and methane are now given.

### Mechanism I

After reactions 1, 2, 12 and 13 have produced  $H^\cdot$  and CS, the following reactions may occur:





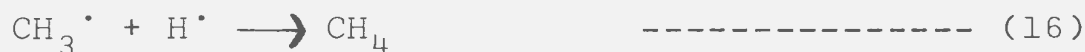
Reaction 14 has recently been proposed in the flash photolysis of methanethiol (1). However, it is difficult to explain its occurrence rather than the much more exothermic reaction



The production of sulphur atoms by a photolytic step may be more likely.

#### Mechanism II

Again reactions 1, 2, 12, and 13 are proposed for the production of  $\text{H}^\cdot$  and  $\text{CS}$  as well as  $\text{CH}_3\text{S}^\cdot$ . Then



Reaction 18 requires some mobility of  $\text{CS}$  in the lattice. If  $\text{CH}_2\text{S}$  is substituted for  $\text{CH}_3\text{S}^\cdot$  the reaction is still

energetically feasible for the production of CS<sub>2</sub>.

It is possible that both of these mechanisms contribute to the formation of carbon disulphide and methane, although mechanism II is sounder thermodynamically.

### The annealing effect

When CH<sub>3</sub><sup>·</sup> radicals were observed in the moist methanethiol experiments, they were found to persist far longer than the CH<sub>3</sub>S<sup>·</sup> radicals upon annealing and, in some cases, the CH<sub>3</sub> signal seemed to show a slight increase. The decay times of CH<sub>3</sub><sup>·</sup> and CH<sub>3</sub>S<sup>·</sup> in the gas phase are known to be comparable (45) and further the present methyl sulphide experiments did not show a longer persistence of the methyl signal. Therefore there is no apparent reason why CH<sub>3</sub><sup>·</sup> should be more stable than CH<sub>3</sub>S<sup>·</sup> in the present methanethiol experiments and the longer persistence of the CH<sub>3</sub><sup>·</sup> signal must be attributed to the formation of more CH<sub>3</sub><sup>·</sup> radicals during the annealing process. This will arise when the mobility of CS in the matrix is increased at the higher temperature thus facilitating the formation of CH<sub>3</sub><sup>·</sup> by



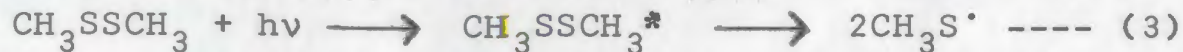
The annealing effect therefore offers strong evidence for mechanism II given above.

Although by no means conclusive, tables 8 and 9 seem to indicate a tendency for the ratio  $\text{CH}_4::\text{CS}_2$  in the products to increase (i) with the use of a low pressure mercury lamp rather than a high pressure lamp, and (ii) when no inert gas matrix was used. If correct, (i) could be due to a larger proportion of the primary photolysis being via C-S cleavage (the weaker bond) with the low pressure lamp. Observation (ii) would be explained by reaction 18 occurring more readily when no isolating matrix was present, since the reacting species would not be so well separated in this case and mobility would not be such a problem. Assuming all  $\text{CH}_3\cdot$  radicals formed lead to methane, the proportion of methane should then be larger than if more  $\text{CH}_3\text{S}\cdot$  radicals were subjected to secondary photolysis by reaction 12.

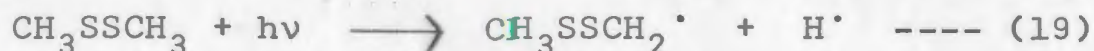
#### Decomposition mechanism of methyl disulphide

#### Production of carriers of the E.S.R. signals

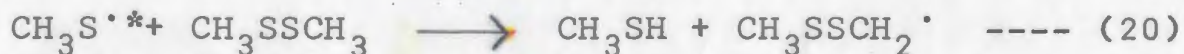
Cleavage of the S-S bond is accepted as the major primary photolytic process in the solid, liquid and gaseous phases (1, 13-18), with the disulphide molecule first being raised to an excited state



The present E.S.R. experiments show a signal attributed to  $\text{CH}_3\text{S}^\cdot$  which is assumed to be produced by reaction 3. Also seen in E.S.R. are three lines which have been attributed to  $\text{CH}_3\text{SSCH}_2^\cdot$ . Whilst this species would arise if any primary photolysis occurred via C-H cleavage



it could also arise by an abstraction reaction involving an excited thiyl radical



It is notable that 253.7-nm radiation at 77K did not produce this three line spectrum (13). Reaction 19 could occur more readily in the present work if an alternative excited state lay a little higher than the excited state entered via 253.7-nm radiation. This higher excited state would have a structure which would lead to C-H cleavage rather than S-S cleavage. The probability of two such excited states lying so close is however not very high. Reaction 20 is also more likely to occur in the present E.S.R. work since the

higher energy radiation will produce more energetic  $\text{CH}_3\text{S}^*$  radicals which will abstract hydrogen atoms more readily. This explanation of the production of  $\text{CH}_3\text{SSCH}_2^*$  is preferred.

Formation of  $\text{CH}_3\text{SH}$ ,  $\text{CS}$  and  $\text{CS}_2$

The infrared matrix experiments clearly show the formation of methanethiol. Reaction 20 is not expected to account for this since the  $\text{CH}_3\text{S}^*$  radicals should be well isolated from substrate molecules and both are too large to be mobile in the matrix. A disproportionation reaction in the cage is preferred.



Both the methanethiol and the thioformaldehyde would be expected to undergo secondary photolysis as discussed under decomposition mechanism of methanethiol.

However it will be noted (tables 8 and 10) that the CS absorption in the disulphide experiments is much less than that in the methanethiol experiments, although more carbon disulphide is formed in the disulphide experiments. This is presumed to be due to two sulphur

containing species being close neighbours in the disulphide experiments. Any CS which is formed will then easily locate a species containing a sulphur atom which can be abstracted without any mobility of CS from its cage being necessary. It is also possible that a species containing two sulphur atoms will form before degradation to CS has occurred. Many infrared absorptions (designated E) were observed in only the disulphide experiments and were therefore probably carried by species which contained two sulphur atoms. Some of these absorptions were relatively intense compared with other absorptions produced by photolysis, perhaps indicating that the most important route to CS<sub>2</sub> is via species containing two sulphur atoms rather than via CS. Further evidence for this type of mechanism possibly arises from the failure to detect CH<sub>3</sub><sup>•</sup> in the E.S.R. and from the failure to make conclusive CH<sub>4</sub> assignments in the infrared. These observations indicate that reaction 18 is of much less importance in the photolysis of the disulphide than in the photolysis of the thiol, and a route to CS<sub>2</sub> via species containing two sulphur atoms is a natural alternative.

## Decomposition mechanism of methyl sulphide

The primary photolytic process upon photolysis of this compound is known to be (1, 18, 19, 20)



Signals attributed to  $\text{CH}_3\text{S}\cdot$  and  $\text{CH}_3\cdot$  were observed in the present E.S.R. experiments. In the argon matrix experiments (and possibly in the pure solid of the E.S.R. experiments) this would be followed by a disproportionation in the 'cage'.



Methane was observed in the infrared, and the thioformaldehyde would be expected to undergo secondary photolysis as described previously.

## The unassigned infrared absorptions

It is now possible to make tentative suggestions of possible carriers of these spectra (table 13). The classification into groups A to F however must be regarded as suspect since (i) in some cases the absorptions are so weak that it is difficult to decide in which experiments they appear, and (ii) some of the weaker absorptions may be produced from these impurities. (iii) two different species may have absorptions at the

same frequency within the limits of experimental error.

Table 13. Tentative suggestions on the origin of unassigned infrared lines.

---

Absorptions designated	Possible carriers
A	$\text{CH}_3\text{S}^{\cdot}$ , $\text{CH}_2\text{S}$ .
B	Species derived from $\text{CH}_3\text{SH}$
D	Same as B or impurity.
E	Species derived from $\text{CH}_3\text{SS}^{\cdot}$ or other species containing two sulphur atoms.
F	Impurity

---

Since  $\text{CH}_3\text{S}^{\cdot}$  and  $\text{CH}_2\text{S}$  are the only species with unassigned absorptions which are suspected to be present in all experiments it is suggested that one or both of these produce the absorptions designated 'A'. The absorptions common to the methanethiol and methyl disulphide experiments (designated 'B') possibly arise from products of methanethiol molecules since the latter are known to be present in both experiments. Two very weak lines (designated 'D') at  $2868 \text{ cm}^{-1}$  and  $3024 \text{ cm}^{-1}$

appear only from methanethiol. It is possible that these did not appear in the disulphide experiments because they were too weak. Alternatively they may arise from impurity since CO was known to be formed in the methanethiol experiment and other oxygen containing species may also be formed.

Many lines appear only in the disulphide experiments and several of them are relatively intense. The only species which are not expected to be formed from the other compounds are species containing two sulphur atoms. These may arise by C-S cleavage in the primary photolytic step (18) or by recombination of two fragments after S-S cleavage has occurred in the primary photolysis. C-S cleavage in the substrate would produce  $\text{CH}_3\text{SS}^\bullet$  from which  $\text{CH}_3\text{SSH}$  or  $\text{CH}_2\text{SS}$  etc. may form. The formation of  $\text{CH}_3\text{SSCH}_2^\bullet$  from the substrate is not considered since (i) C-H cleavage as a primary photolysis is unlikely, and (ii) the abstraction reaction 20 is not expected in the argon matrix since  $\text{CH}_3\text{S}^\bullet$  should be well separated from the substrate molecules and is not expected to be mobile. One absorption at  $2090\text{ cm}^{-1}$  appears only in the methyl sulphide experiments. This may be due to an impurity.

## Rotation effect on E.S.R. spectra from methanethiol

The change in the spectrum of thiyl radicals in methanethiol is ascribed to the radicals having a preferred orientation in the sample. If radicals have preferred orientations in a single crystal, the spectra will vary with the orientation of the crystal in the magnetic field in a manner which reflects the anisotropy in the  $g$ - and hyperfine tensors. Since the present samples were polycrystalline, such an effect would not normally be expected, but consideration of the following points may be of value. A single crystal of methanethiol (at least in its high temperature phase) is known to have all the C-S bonds close to the same direction (24). Also since the methyl thiyl radical is large, it is unlikely to move significantly from the position and orientation of its parent molecule. Accordingly the radicals should have preferred directions in a single crystal and an orientation effect is expected in that case. Photolysis in the solid state is sometimes arrested because one or more of the products may absorb the actinic light more effectively than the parent material, thus acting as an "inner filter" (46). Both  $\text{CH}_3\text{S}^\bullet$  and  $\text{CH}_2\text{S}$  are known to absorb in the ultraviolet (45) so that S-H bond fission in the substrate may well

occur only at the surface of the solid. This view is supported in the present experiments in that the methanethiyl spectrum reached a maximum intensity after approximately twenty minutes photolysis (the intensity could be increased further by photolysing new positions on the sample). The photolysis lamp was focussed to illuminate only a small area of the sample. If this surface area showed a preferred orientation of the crystals, or if only a few crystals received the bulk of the light energy, an orientation effect may be observed.

#### Suggestions for further work

It may be possible to obtain more specific assignments of some of the infrared absorptions by checking on the relative rates of decay of the different absorptions when the matrix was subjected to various annealing processes. An easier way to obtain more specific assignments may be to extend the work to different systems - e.g. photolysis of (i)  $\text{CH}_4$  and  $\text{COS}$ , (ii)  $\text{CH}_2\text{N}_2$  and  $\text{COS}$ , (iii)  $\text{CS}_2$  and  $\text{H}_2\text{S}$  with or without an argon matrix.

If a suitable inert matrix could be found for  $\text{CH}_3\text{SH}$  in the E.S.R. experiments (or better still if the argon

matrix techniques could be used with the E.S.R. spectrometer) better correlation between the E.S.R. and infrared data might be available.

Finally an extended use of isotopes such as  $C^{13}$  (E.S.R. and infrared) and  $S^{33}$  (E.S.R.),  $S^{34}$  (infrared) would help in assigning further spectra and in confirming some assignments already made.

## BIBLIOGRAPHY

1. A.B. Callear and D.R. Dickson. Trans. Faraday Soc. 66, 1987 (1970).
2. D.R. Johnson and F.X. Powell. Science. 169, 679 (1970).
3. A.J. Barnes and H.E. Hallam. Quart. Rev. 23, 392 (1969).
4. A.M. Bass and H.P. Broida. Formation and Trapping of Free Radicals. Academic Press, New York (1960).
5. J.G. Calvert and J.N. Pitts, Jr. Photochemistry. John Wiley, New York (1967).
6. K.J. Rosengren. Acta Chem. Scand. 16, 1414 (1962).
7. G.P. Sturm Jr. and J.M. White. J. Chem. Phys. 50, 5035 (1969).
8. R.P. Steer and A.R. Knight. J. Phys. Chem. 72, 2145 (1968).
9. R.P. Steer, B.L. Kalra and A.R. Knight. J. Phys. Chem. 71, 783 (1967).
10. R.P. Steer and A.R. Knight. Can. J. Chem. 46, 2878 (1968).
11. S. Yamashita and F.P. Lossing. Can. J. Chem. 46, 2925 (1968).
12. D.H. Volman, J. Wolstenholme and S.G. Hadley. J. Phys. Chem. 71, 1798 (1967).

13. J.J. Windle, A.K. Wiersema and A.L. Tappel. J. Chem. Phys. 41, 1996 (1965).
14. F.K. Truby, D.C. Wallace and J.F. Hesse. J. Chem. Phys. 42, 3845 (1965).
15. P.M. Rao, J.A. Copeck and A.R. Knight. Can. J. Chem. 45, 1369 (1967).
16. K. Sayamol and A.R. Knight. Can. J. Chem. 46, 999 (1968).
17. P.M. Rao and A.R. Knight. Can. J. Chem. 46, 2462 (1968).
18. A. Jones, S. Yamashita and F.P. Lossing. Can. J. Chem. 46, 833 (1968).
19. L. Horner and J. Dörge. Tetrahedron Letters. 12, 757 (1963).
20. B. Milligan, D.E. Rivett and W.E. Savige. Aust. J. Chem. 16, 1020 (1963).
21. I.W. May and E.L. Pace. Spectrochim. Acta. 24A, 1605 (1968).
22. R.J. Abraham, J.A. Pople and H.J. Bernstein. Can. J. Chem. 36, 1302 (1958).
23. H. Russell, D.W. Osbourne and D.M. Yost. J. Am. Chem. Soc. 64, 165 (1942).
24. I.W. May and E.L. Pace. Spectrochim. Acta. 25A, 1903 (1969).

25. T. Kojima. J. Phys. Soc. Japan. 15, 1248 (1960).
26. R.W. Kibb. J. Chem. Phys. 23, 1736 (1955).
27. N. Solimene and B.P. Dailey. J. Chem. Phys. 23, 124 (1955).
28. See for example G. Herzberg. Molecular Spectra and Molecular Structure. II Infrared and Raman Spectra of Polyatomic Molecules. D. Van Nostrand, Princeton. (1968).
29. A.B. Harvey and M.K. Wilson. J. Chem. Phys. 45, 678 (1966).
30. M. Faulk and E. Whalley. J. Chem. Phys. 34, 1554 (1961).
31. E.B. Wilson Jr., J.C. Decius and P.C. Cross. Molecular Vibrations. McGraw Hill, New York (1955).
32. M. Davies ed. Infrared Spectroscopy and Molecular Structure. Elsevier, Amsterdam (1963).
33. D.A. Stiles, W.J.R. Tyerman, O.P. Strausz and H.E. Gunning. Can. J. Chem. 44, 1677 (1966).
34. T. Henriksen. J. Chem. Phys. 37, 2189 (1962).
35. F.K. Truby, D.C. Wallace and J.E. Hesse. J. Chem. Phys. 42, 3845 (1965).
36. A. Torikai, S. Sawada, K. Fueki and Z. Kuri. Bull. Chem. Soc. Japan. 43, 1617 (1970).

37. D.A. Stiles, W.J.R. Tyerman, O.P. Strausz and H.E. Gunning. *Can. J. Chem.* 44, 2149 (1966).
38. W.G. Hodgson, S.A. Buckler and G. Peters. *J. Am. Chem. Soc.* 85, 543 (1963).
39. A. Horsfield, J.R. Morton and D.H. Whiffen. *Mol. Phys.* 4, 169 (1961).
40. P.B. Ayscough and C. Thompson. *Trans. Faraday Soc.* 58, 1477 (1962).
41. R. Steudel. *Z. anorg. allg. Chem.* 361, 180 (1968).
42. G. Grieg and J.C.J. Thynne. *Trans. Faraday Soc.* 62, 379 (1966).
43. A. Jones and F.P. Lossing. *J. Phys. Chem.* 71, 411 (1967).
- D.H. Fine and J.B. Westmore. *Can. J. Chem.* 48, 395 (1970).

Heats of formation not listed in these papers were taken from Janaf Thermochemical Tables. U.S. Department of Commerce (1965).

44. D.A. Stiles, R. Kewley, O.P. Strausz and H.E. Gunning. *Can. J. Chem.* 43, 2442 (1965).
45. A.B. Callear, J. Connor and D.R. Dickson. *Nature*, 221, 1238 (1969).
46. P.W. Atkins and M.C.R. Symons. *The Structure of Inorganic Radicals*. Elsevier, Amsterdam, page 40 (1967).

47. H.C. Allen and P.C. Cross. Molecular Vib-Rotors.  
Wiley, New York (1963).





